Quantum computing

Lecture 1

Hélène Perrin

January 24, 2021

Introduction

Topic of the course: realization of experimental platforms for quantum computation or quantum simulation

- Mastering single quantum objects = 'qubits' and use entanglement: first pioneered with photons (quantum optics), then atoms and ions, and finally with solid state devices: superconducting transmon qubits, spin qubits...
- Realize single qubit gates (rotations on the Bloch sphere) and two-qubit gates (preparing entangled states)
- A common formalism valid for all platforms: quantum computation (see Perola Milman's lectures)

Introduction

Topic of the course: realization of experimental platforms for quantum computing or quantum simulation

- A common problem to face: decoherence. Challenge: increase the number of operations within the decoherence time.
- Possible trade-off: Development of error correction schemes with several physical qubits to encode a single logical qubit.
- No universal quantum computer available yet! Rather quantum simulators with various experimental advantages and limitations. The best choice depends on the problem to address.

Criteria for a quantum computer

David DiVincenzo proposed five criteria that a quantum computer should fulfill:

- A scalable physical system with well characterised qubits.
- The ability to initialize the state of the qubits to a simple fiducial state.
- Long relevant decoherence times.
- A universal set of quantum gates.
- A qubit-specific measurement capability.

The criteria are less stringent on quantum simulators (especially on scalability and universality).

The platforms

Experimental platforms studied in this course (tentative list)

- Trapped ions
- Transmon (superconducting) qubits
- NMR qubits
- Electron spins in quantum dots
- Electron spins in silicium
- Photons
- Rydberg atoms
- Ultracold atoms in optical lattices

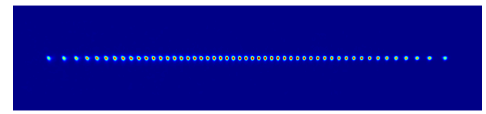

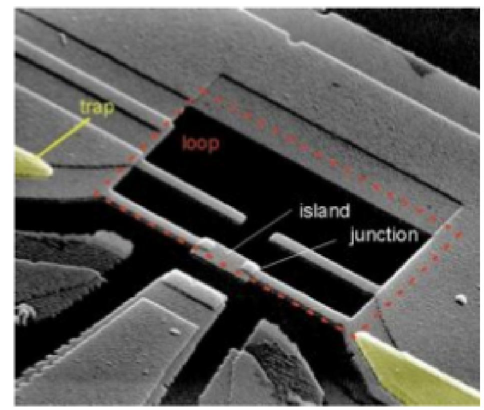

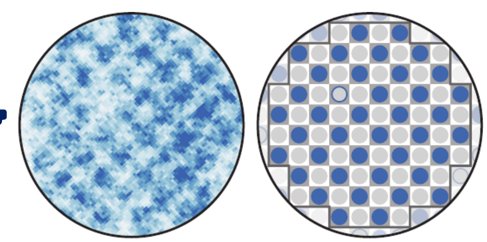

Outline of this course

Lecture 1: Quantum computation with trapped ions

1. Trapping charged particles
2. Laser manipulation of trapped ions
3. Coupling ions via phonons
4. Example of quantum algorithms performed with trapped ions

Outline of this course

Lecture 2: Quantum computation with transmon qubits

1. The superconducting transmon qubit
2. Manipulation of a single qubit with microwave fields
3. Two qubit gates
4. Example of quantum algorithms performed with transmon qubits

Outline of this course

Lecture 3: Other quantum computation platforms

1. NMR in molecules
2. Spins in quantum dots
3. Silicium qubits
4. Photons

Outline of this course

Lecture 4: Quantum simulation with neutral atoms

1. Rydberg atoms in micro-traps
2. Quantum gases in optical lattices
3. Quantum gases in the bulk

Bibliography

- lecture notes by John Preskill
  `http://www.theory.caltech.edu/people/preskill/ph229/`
- M. Nielsen and I. Chuang, *Quantum Computation and Quantum Information*, Cambridge 2010
- G. Benenti, G. Casati and G. Strini, *Principles of Quantum Computation and Information*, World Scientific 2007
- C. Cohen-Tannoudji and D. Guéry-Odelin, *Advances in atomic physics: an overview*, World Scientific 2012 (or the French version, Hermann 2016)
- S. Haroche and J.-M. Raimond, *Exploring the quantum*, OUP 2006
- C. Champenois, *Trapping and cooling of ions*, Les Houches lecture notes
  `https://cel.archives-ouvertes.fr/cel-00334152`
- C. Bruzewicz, J. Chiaverini, R. McConnell, and J. Sage, *Trapped-Ion Quantum Computing: Progress and Challenges*, `https://arxiv.org/abs/1904.04178`
- M. Devoret, A. Walraff and J. Martinis, *Superconducting qubits: a short review*, `https://arxiv.org/abs/cond-mat/0411174`

Lecture 1: Quantum computation with trapped ions

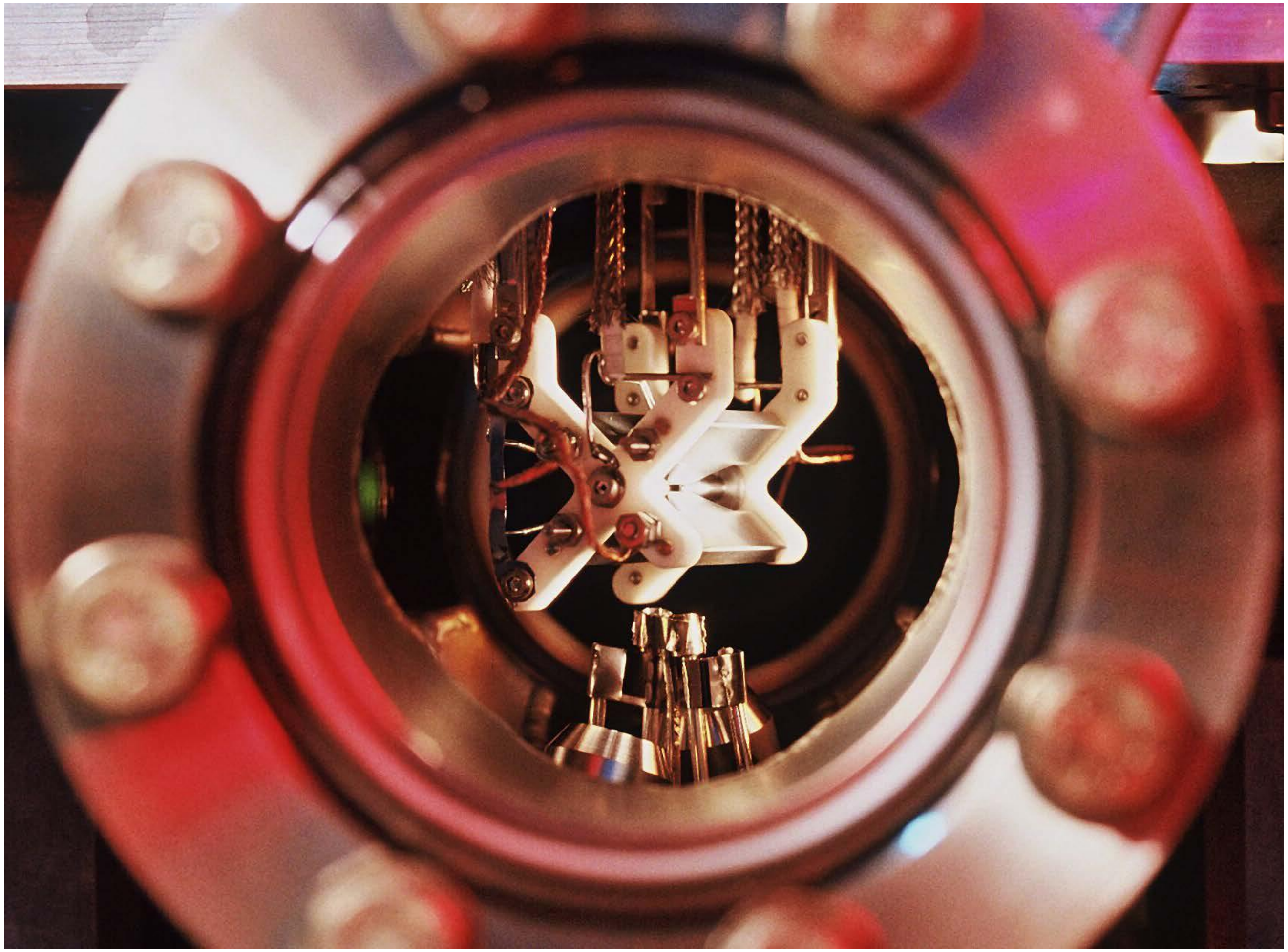

Outline

Introduction

Trapping charged particles

- Penning trap
- Paul trap
- Quantized motion in the trap

Laser manipulation of trapped ions

- Reminder on atom-light interaction
- Laser cooling to the ground state
- Qubit manipulation and detection

Coupling ions via phonons

- Phonons as control qubit
- Center of mass mode of an ion chain
- Phonon-mediated two-qubit gates

Example of a quantum algorithm with trapped ions

Trapping charged particles

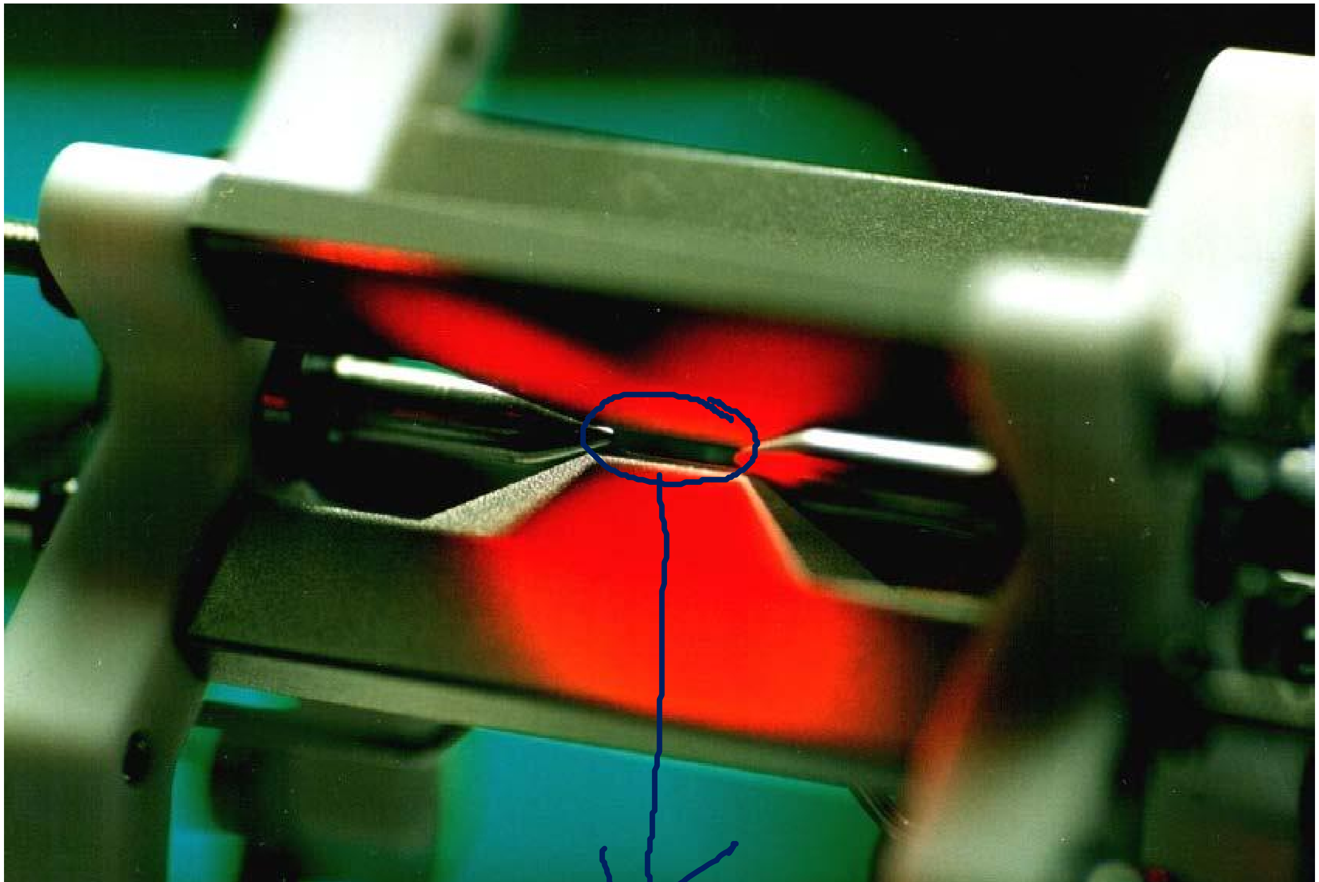

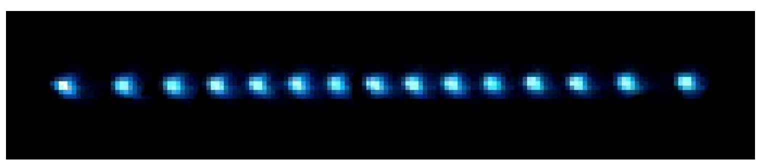

Characteristics of a 'good' ion trap

Objective: ability to manipulate the internal degree of freedom of single ions (qubit) and couple ions for two-qubit gates to satisfy the DiVincenzo criteria.

electric traps

- trap should not affect the qubit transition
  $\Rightarrow$ confinement relying on the charge itself
- absolute control on the external degree of freedom
  $\Rightarrow$ tight trap and cooling to the ground state

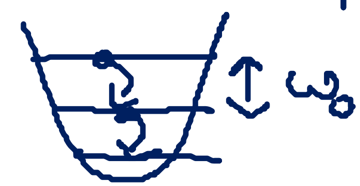

- addressability of individual ions
  $\Rightarrow$ separation larger than the resolution (esp. for optical transitions)
- avoid decoherence
  $\Rightarrow$ controlled environment (ultra-high vacuum, low noise, etc.)

Trapping charged particles with electric fields

A static electric field cannot confine a charged particle ($\nabla \cdot E = 0$ or $\Delta U = 0$). We can only get two directions trapped and the other antitrapped, with a potential between two conductors of the form:

$$U(x, y, z) = \frac{1}{2} M\omega^2 \left(\frac{x^2 + y^2}{2} - z^2 \right).$$

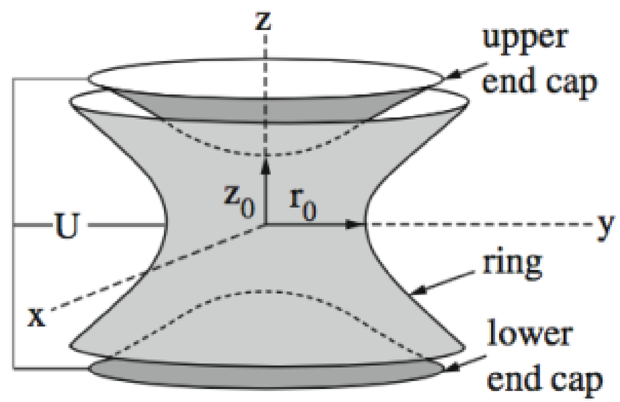

To stabilize the particle in 3D, there are two options:

- Add a magnetic field: Penning trap
- Make the electric field time-dependent: Paul trap

The Penning trap

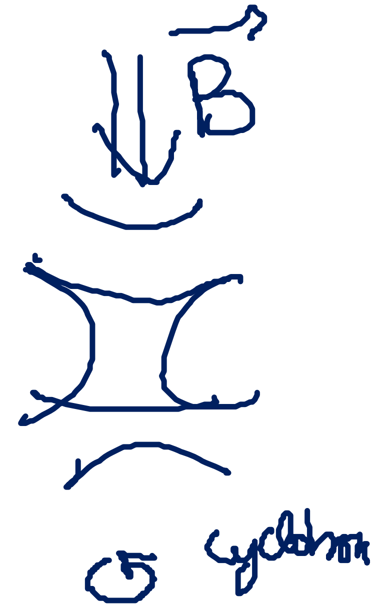

Electric confinement along z

$$U(x,y,z) = \frac{1}{2}M\omega^2\left(-\frac{x^2+y^2}{2}+z^2\right).$$

Magnetic confinement in the plane

Magnetic field B alonz z with a cyclotron frequency $\omega_c = qB/M$ much larger than ω. The in-plane motion is decomposed into a fast rotation at $\sim \omega_c$ and a slow oscillation at the magnetron frequency ω_m

$$\omega_m \simeq \frac{\omega^2}{2\omega_c} \ll \omega \ll \omega_c$$

Trajectory in a Penning trap

Typical trajectory

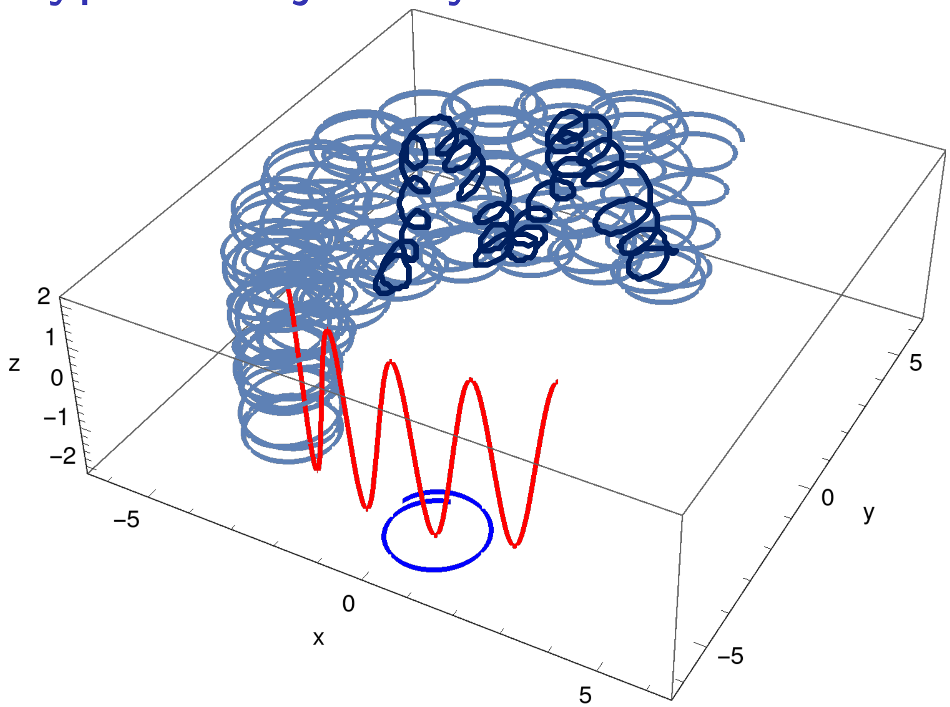

Main usages

- Trapping single particles for metrology (measurement of mass ratio, measurement of $g-2$ of a single electron. . .)
- Study ion crystals

Drawback for quantum computation:

Lower trapping frequency of the magnetron motion (typ. 10-100 kHz).

The Paul trap

Key idea: alternate the voltage fast enough ($\Omega \gg \omega$) such that the particle remains trapped in the time-averaged potential.

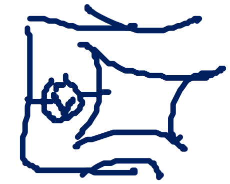

$M\vec{a} = -\vec{\nabla} U = \vec{F}$

$$U(x,y,z,t) = \frac{1}{2}M\omega^2\left(-\frac{\overbrace{x^2+y^2}^{=\rho^2}}{2}+z^2\right)\cos(\Omega t).$$

Decompose the motion into fast + slow: $\mathbf{r} = \underbrace{\overset{\sim\Omega}{\mathbf{r}_f}} + \underbrace{\overset{\ll\Omega}{\mathbf{r}_s}}$ with $r_f \ll r_s$. On the fast scale Ω, $\mathbf{r}_s$ is fixed:

$\vec{r}_f = \rho_f \vec{e}_\rho + \rho_z \vec{e}_z$

$$\ddot{\mathbf{r}}_f = -\frac{\omega^2}{2}\begin{pmatrix}-\rho_s\\ 2z_s\end{pmatrix}\cos(\Omega t) \Rightarrow \mathbf{r}_f = \frac{\omega^2}{2\Omega^2}\begin{pmatrix}-\rho_s\\ 2z_s\end{pmatrix}\cos(\Omega t).$$

Now the slow motion obeys the time-averaged equation:

$$\ddot{\mathbf{r}}_s = -\frac{\omega^2}{2}\left\langle\begin{pmatrix}\overset{\sim\Omega}{-\rho_f\cos(\Omega t)}\\ 2z_f\cos(\Omega t)\end{pmatrix}\right\rangle = -\frac{\omega^4}{8\Omega^2}\begin{pmatrix}\rho_s\\ 2z_s\end{pmatrix}.$$

The Paul trap: average potential

$\omega_\perp = \omega \underbrace{\frac{\omega}{\Omega}}_{\text{small}} \ll \omega$

Final potential for the slow motion:

$$V(x_s, y_s, z_s) = \frac{M\omega^4}{16\Omega^2}\left(x_s^2 + y_s^2 + 4z_s^2\right).$$

$\Rightarrow$ Harmonic trap with frequencies $\omega_\perp = \omega^2/2\sqrt{2}\Omega$ and $\omega_z = 2\omega_\perp$.

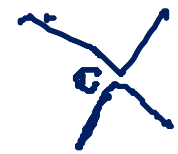

Remarks: radio-frequency 100 MHz – 10 GHz

- Ω is in the rf domain, Paul traps are also called rf traps.
- $\omega_{z,\perp} \ll \omega \ll \Omega$ so it's important to start with a very steep electric potential (easier for small-scale traps).

- $V(\mathbf{r}_s) = M\mathbf{v}_f^2/2$: the trap relies on the kinetic energy of the micromotion. This motion is hence more important for a particle far from the center. It vanishes at the center where the fields cancel.
- The stability of the trap is valid only under some assumptions. See e.g. the Mathieu stability diagramme in the course of C. Champenois.

The Paul trap: 3D vs linear

The Paul trap can be implemented in a linear quadrupole version, ideal to confine a linear ion chain (a static field is added to trap the z motion):

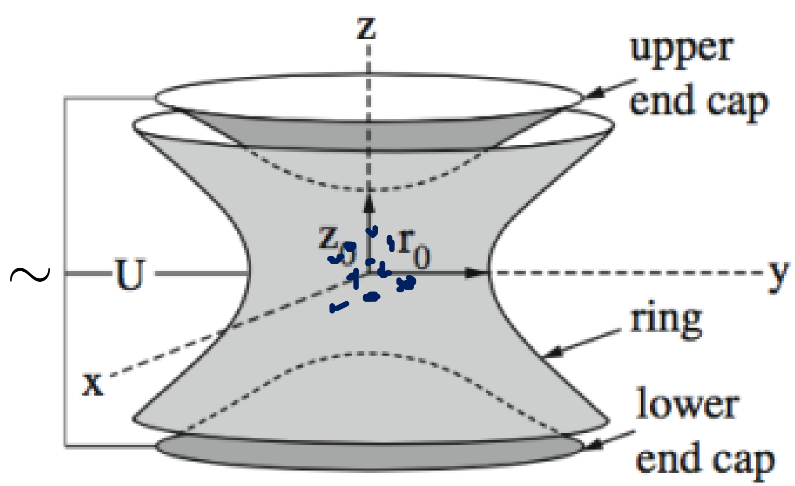

3D Paul trap

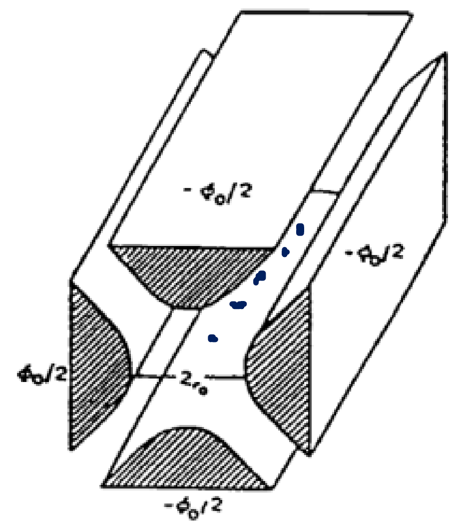

Linear Paul trap

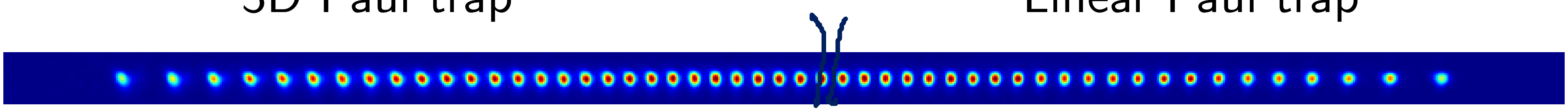

Linear Paul traps are ideal to confine many ions while limiting the micromotion (ion chain at the center $x = y = 0$). They can be made smaller $\Rightarrow$ reach higher frequencies ($\sim$ 10 MHz). They are used in optical metrology of time or quantum optics and quantum computing.

Linear Paul trap in practice

End caps with positive voltage $U_{\text{end}} > 0$ to confine the weak (x) axis.

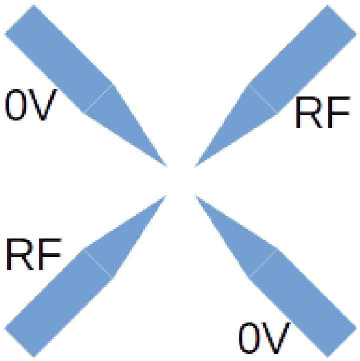

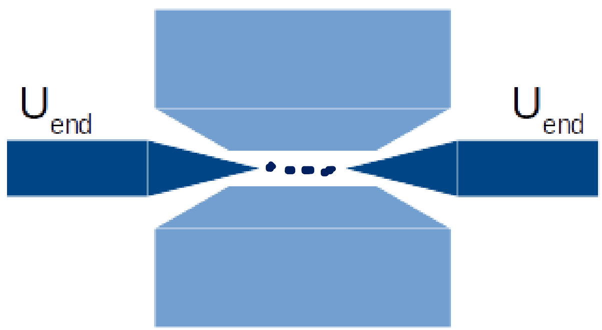

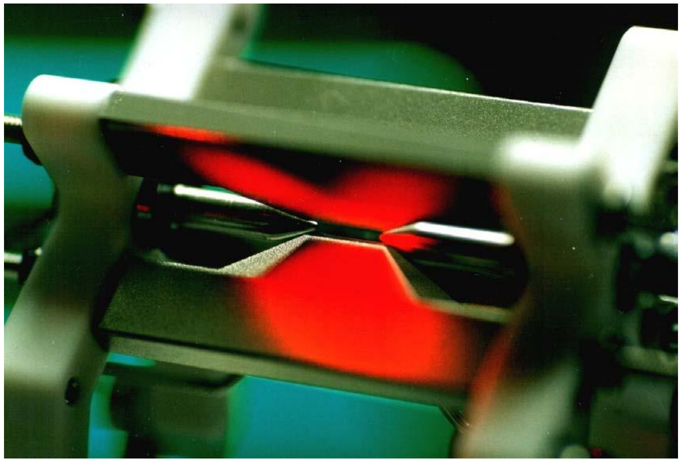

Innsbruck linear Paul trap (2000)

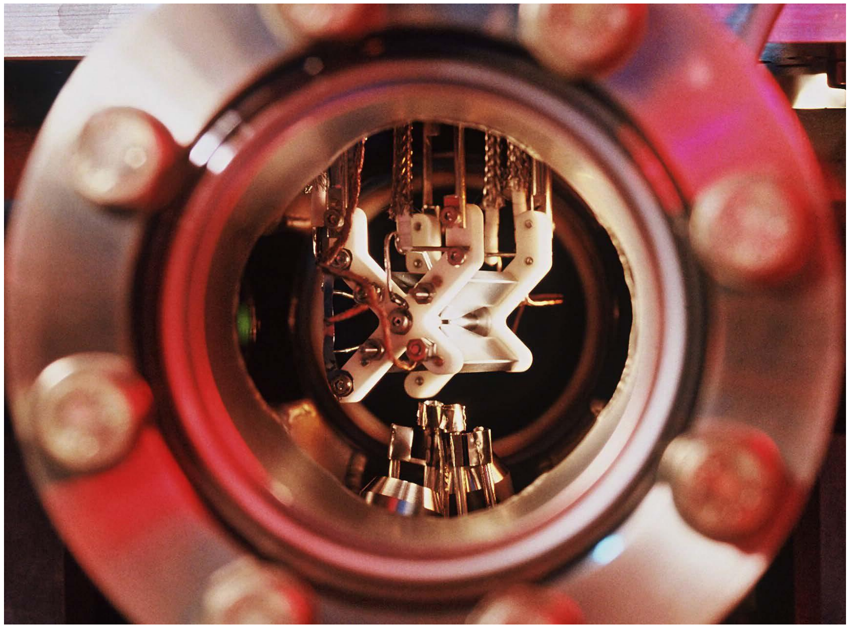

ion trap inside the vacuum chamber

Linear Paul trap in practice

The end caps can be placed at the end of the ground rods to improve optical access.

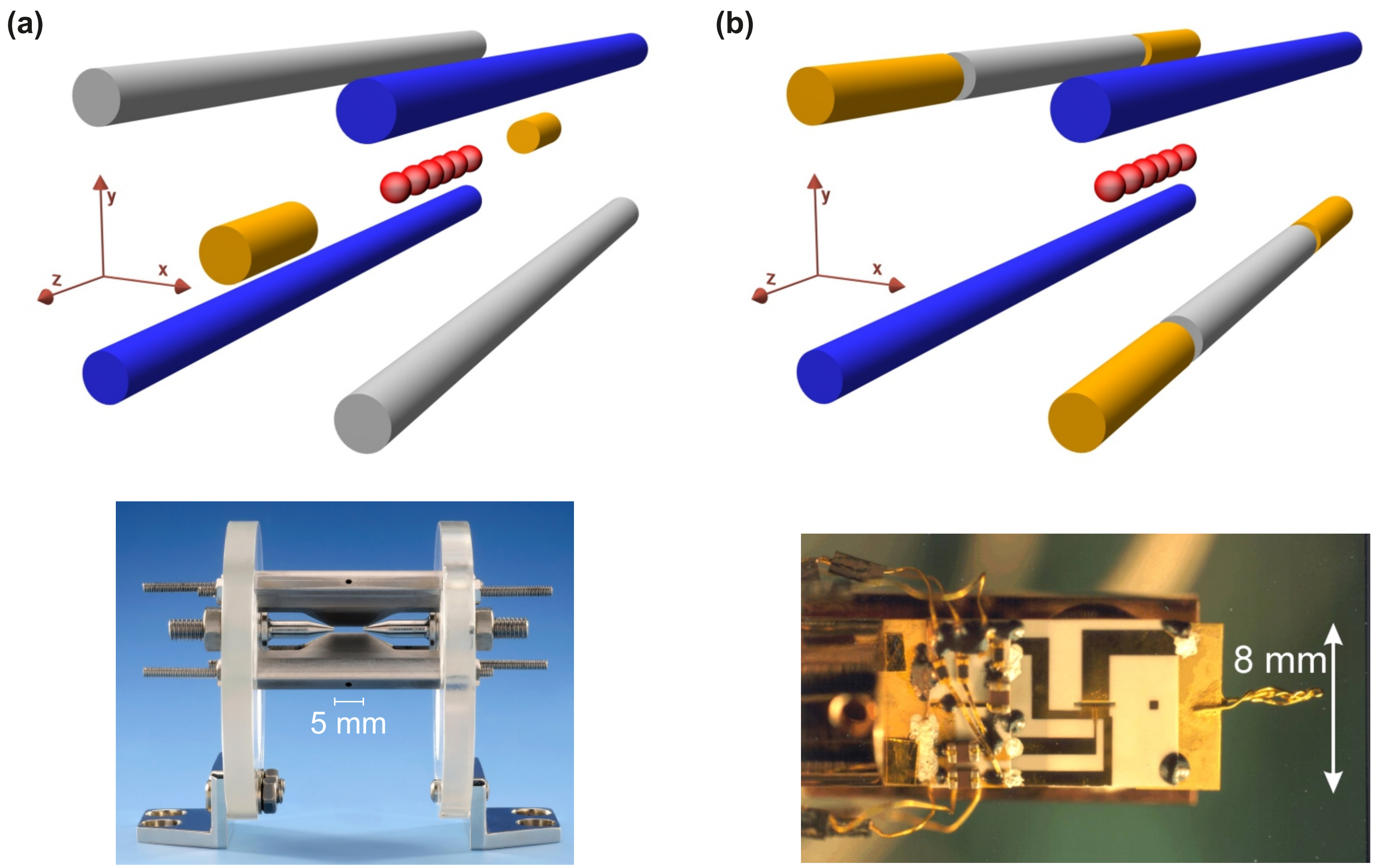

Figure from Ludlow et al., RMP **87**, 637 (2015)

Going small: Surface ion traps

Surface ion trap design of the Boulder group (IonQ company, Chris Monroe). 80 atomic $^{171}Yb^{+}$ ions.

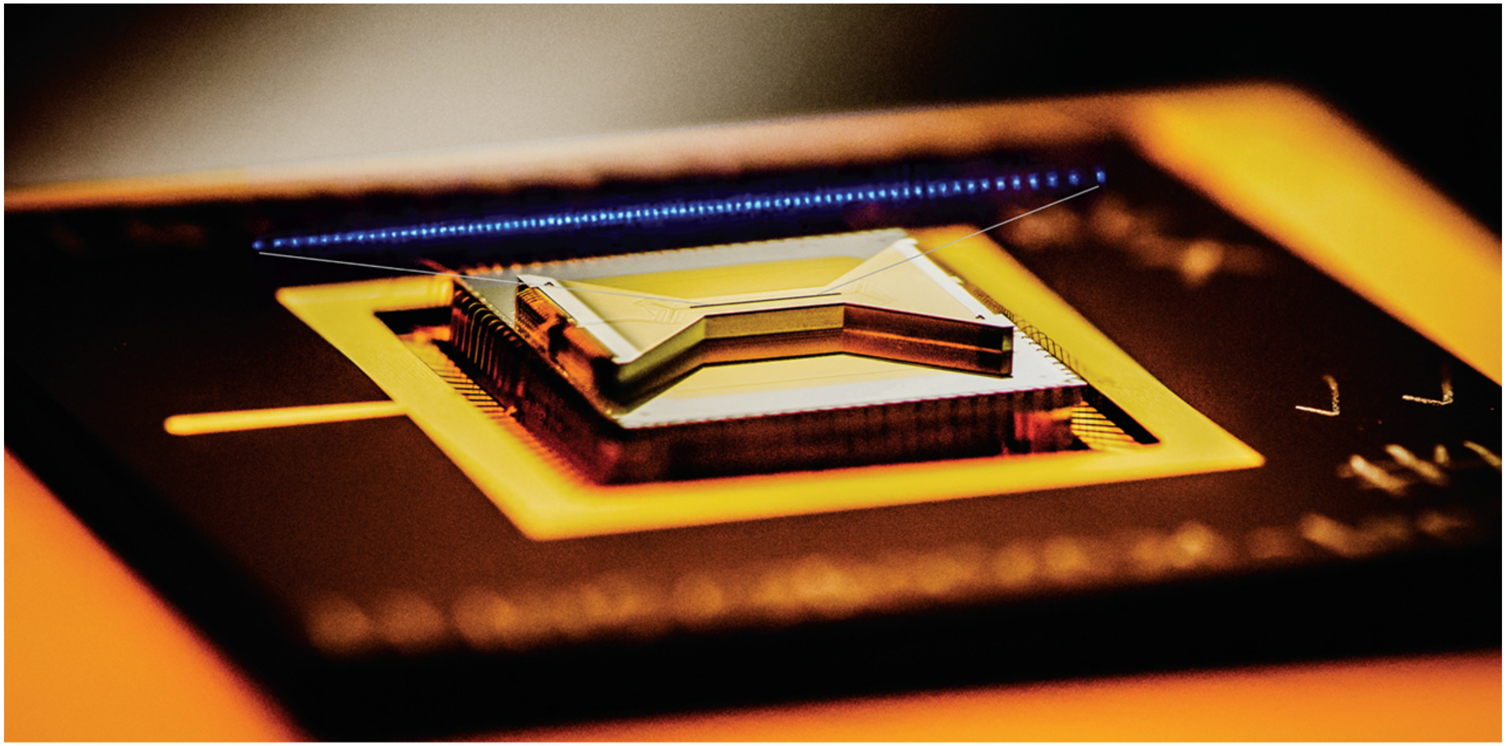

Figure from Monroe et al., Science **364**, 440 (03 May 2019)

Trapped ion: classical vs quantum motion

Consider a harmonic trap with frequency ω_0 along a direction x. Two regimes depending on the ion(s) temperature:

- $k_B T \gg \hbar\omega_0$: Many trap levels are populated, the motion can be described classically with position $\mathbf{r}$ and velocity $\mathbf{v}$.
- $k_B T \ll \hbar\omega_0$: The atomic motion is quantum mechanical. Hamiltonian of the harmonic oscillator:

$$H_{\rm ext} = \frac{\hat{p}^2}{2m} + \frac{1}{2} m\omega_0^2 \hat{x}^2 \qquad \text{with} \qquad [\hat{x}, \hat{p}] = i\hbar.$$

Ground state has a position rms width x_0 and a momentum rms width p_0

$$x_0 = \sqrt{\frac{\hbar}{2m\omega_0}} \qquad p_0 = \sqrt{\frac{\hbar m\omega_0}{2}}$$

such that $x_0 p_0 = \hbar/2$.

Trapped ion: classical vs quantum motion

Trapped ion: classical vs quantum motion

Consider a harmonic trap with frequency ω_0 along a direction x. Two regimes depending on the ion(s) temperature:

- $k_B T \gg \hbar\omega_0$: Many trap levels are populated, the motion can be described classically with position $\mathbf{r}$ and velocity $\mathbf{v}$.
- $k_B T \ll \hbar\omega_0$: The atomic motion is quantum mechanical. Hamiltonian of the harmonic oscillator: $a = \frac{1}{2}\left(\frac{\hat{x}}{x_0} + i\frac{\hat{p}}{p_0}\right)$

$$H_{\text{ext}} = \frac{\hat{p}^2}{2m} + \frac{1}{2}m\omega_0^2\hat{x}^2 = \hbar\omega_0\left(\hat{a}^\dagger\hat{a} + \frac{1}{2}\right)$$

Eigenstates $|n\rangle_{\text{ph}}$ with energies $E_n = \left(n + \frac{1}{2}\right)\hbar\omega_0$.
$\hat{a}$ and $\hat{a}^\dagger$, such that $\left[\hat{a}, \hat{a}^\dagger\right] = 1$, are annihilation and creation operators of vibrations in the trap = phonons.

$$\hat{a}\,|n\rangle_{\text{ph}} = \sqrt{n}\,|n-1\rangle_{\text{ph}} \qquad \hat{a}^\dagger\,|n\rangle_{\text{ph}} = \sqrt{n+1}\,|n+1\rangle_{\text{ph}}$$

$$\hat{x} = x_0\left(\hat{a} + \hat{a}^\dagger\right) \qquad \text{with} \qquad x_0 = \sqrt{\frac{\hbar}{2m\omega_0}}.$$

Laser manipulation of trapped ions

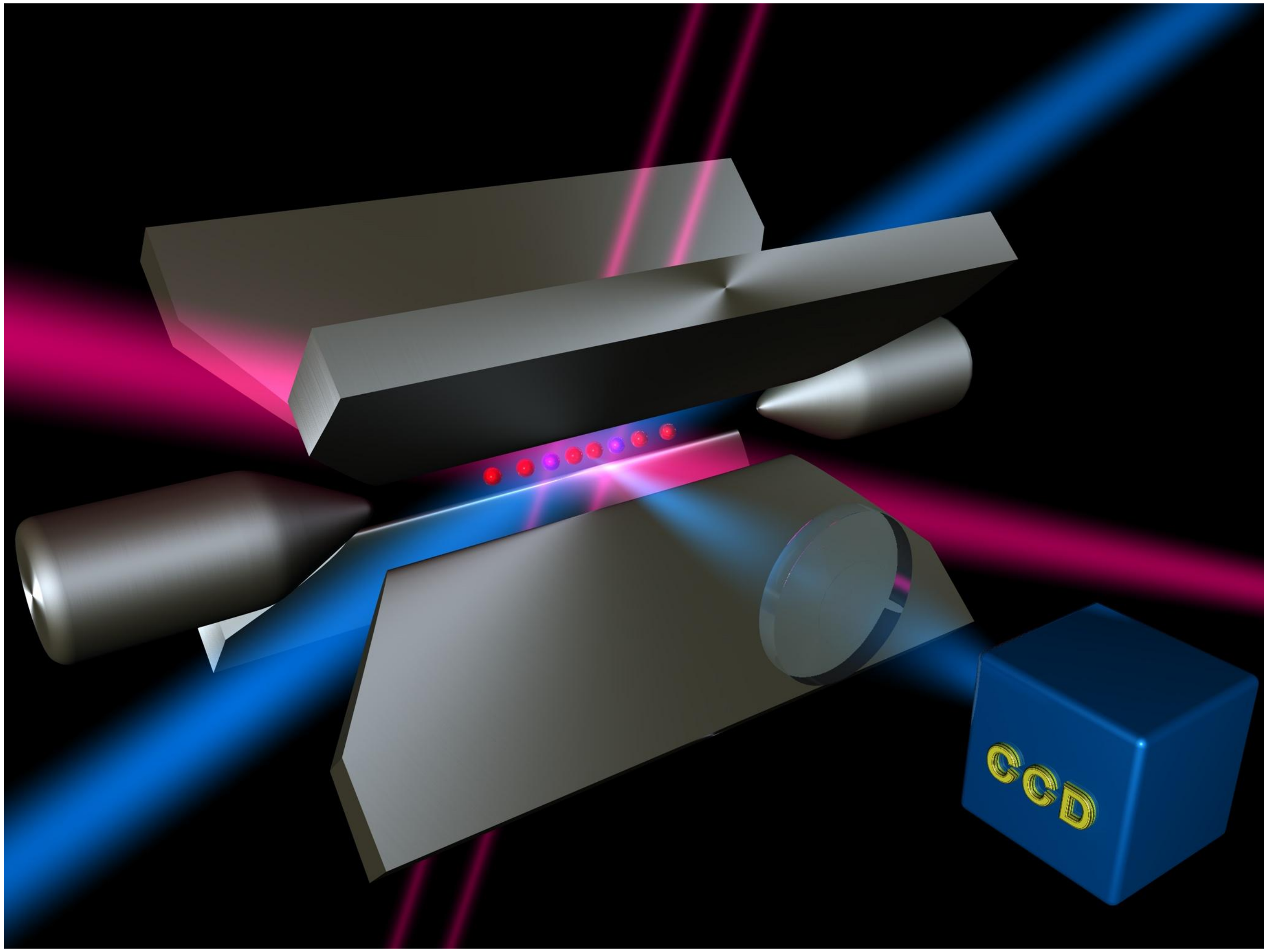

Laser manipulation of trapped ions

Laser manipulation is essential to quantum computation with trapped ions. It serves to

- Cool the external motion (the **phonons**) to the trap ground state (two-step cooling: Doppler + resolved sideband cooling)
- Prepare the initial (internal) state of the qubit
- Perform single- or two-qubit gates
- Read the qubit state

Typical level structure

Ions used for quantum computation as well as clocks are typically alkaline earth atoms (Be^+, Mg^+, Ca^+, Sr^+) or ytterbium Yb^+.

They present a **short lived** excited state $|e\rangle$ of width Γ (ex: $P_{3/2}$) strongly coupled by an electric dipole transition to the ground state $|g\rangle$ (ex: $S_{1/2}$) which can be used for laser Doppler cooling + weaker transitions to **long-lived states** (ex: coupling to $D_{5/2}$ state $|d\rangle$) useful for resolved sideband cooling or gate operations.

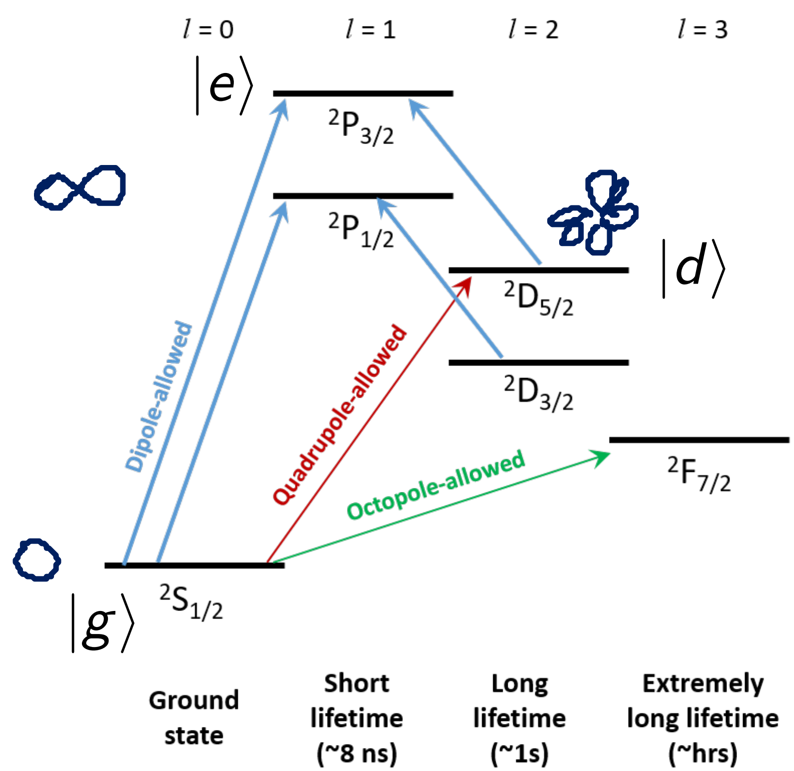

Figure from Bruzewicz et al.

Focus on a two-level system

- Interaction between an atom or ion and nearly resonant light with a particular transition $g \to e$.
- Focus on a two-level system with ground state $|g\rangle$ and excited state $|e\rangle$: $H_0 = \hbar\omega_{eg}/2\,[|e\rangle\langle e| - |g\rangle\langle g|]$.
- All other levels can be ignored
- This two-level system maps onto a 1/2-spin:

$$H_0 = \frac{\hbar\omega_{eg}}{2}\sigma_z \qquad \text{with} \quad \sigma_z = \begin{pmatrix} 1 & 0 \\ 0 & -1 \end{pmatrix}.$$

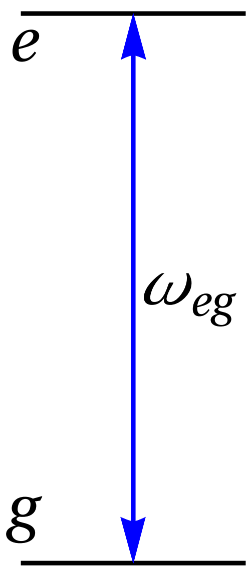

- When the atomic motion is relevant (e.g. for cooling) the ion hamiltonian reads

$$H_{\text{ion}} = H_0 + \frac{\hat{\mathbf{p}}^2}{2m} + V_{\text{trap}}(\hat{\mathbf{r}})$$

treated classically or quantum mechanically depending on temperature T.

Reminder on atom-light interaction (semi-classical)

Atom at position **r** coupled to a monochromatic field at ω

- Internal state Hamiltonian: $H_0 = \frac{\hbar\omega_{eg}}{2}\left[|e\rangle\langle e| - |g\rangle\langle g|\right] = \frac{\hbar\omega_{eg}}{2}\sigma_z$.
- Interaction Hamiltonian in the dipolar approximation:

$\vec{e}$ $\vec{D} = q\vec{R}_e$

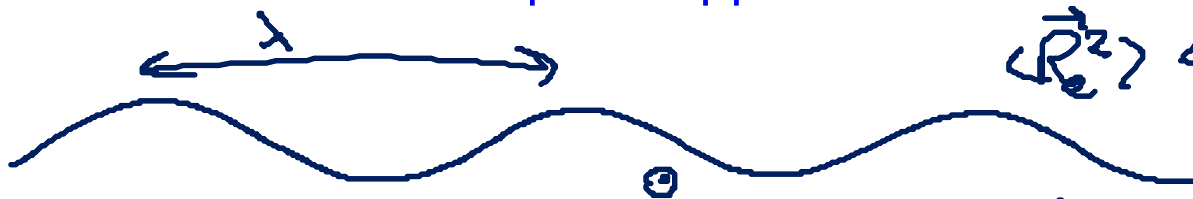

$\langle \vec{R}_e^2 \rangle \ll \lambda^2$

$$H = \frac{(\vec{p} - q\vec{A}(\vec{R}_e,t))^2}{2m_e} + \underbrace{qU(\vec{R}_e)}_{\text{int. with nucleus}} + qV(\vec{R}_e)$$

$$\vec{A}(\vec{R}_e,t) \simeq \vec{A}(\vec{0},t)$$

$$V(\vec{R}_e) \simeq V(\vec{0}) + \vec{R}_e\cdot\vec{\nabla}V$$

$$H = H_0 - \frac{q}{m_e}\vec{p}\cdot\vec{A}(0) + q\cancel{V(\vec{0})} + \underbrace{q\vec{R}_e\cdot\vec{\nabla}V}_{-q\vec{R}_e\cdot\vec{E}(\vec{0},t) - q\vec{R}_e\cdot\frac{\partial\vec{A}}{\partial t}}$$

$$\vec{E} = -\frac{\partial\vec{A}}{\partial t} - \vec{\nabla}V$$

$$\chi = -\vec{r}\cdot\vec{A}(\vec{0},t)$$
$$\vec{A} \to \vec{A} + \vec{\nabla}\chi$$
$$V \to -\frac{\partial\chi}{\partial t} + V$$

$$\searrow \quad H_I = -\vec{D}\cdot\vec{E}$$

Reminder on atom-light interaction (semi-classical)

Atom at position $\mathbf{r}$ coupled to a monochromatic field at ω

- Internal state Hamiltonian: $H_0 = \frac{\hbar\omega_{eg}}{2}\left[|e\rangle\langle e| - |g\rangle\langle g|\right] = \frac{\hbar\omega_{eg}}{2}\sigma_z$.
- Interaction Hamiltonian in the dipolar approximation:

$$\boxed{H_I = -\hat{\mathbf{D}} \cdot \mathbf{E}(\hat{\mathbf{r}}, t)}$$

- $\langle s|\,\hat{\mathbf{R}}_e\,|s\rangle = 0$ in an atomic state s of well-defined parity $\Rightarrow$ Dipole operator $\hat{\mathbf{D}} = q\hat{\mathbf{R}}_e$ is purely off-diagonal in the $\{|g\rangle, |e\rangle\}$ basis:

$$\hat{\mathbf{D}} = \mathbf{d}\,|e\rangle\langle g| + \mathbf{d}^*\,|g\rangle\langle e| = \mathbf{d}\sigma_+ + \mathbf{d}^*\sigma_-$$

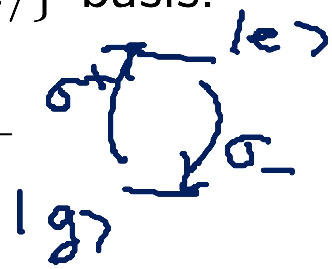

and cancels if $|e\rangle$ and $|g\rangle$ have the same parity.

- Simple case: real dipole $\mathbf{d}$, linearly polarized plane wave:
$\hat{\mathbf{D}} = \mathbf{d}(\sigma_+ + \sigma_-)$
$\mathbf{E}(\mathbf{r}, t) = \mathbf{E}_0\cos(\omega t + \varphi - \mathbf{k}\cdot\mathbf{r}) = \mathcal{E}_0\mathbf{e}_x\cos(\omega t + \varphi - \mathbf{k}\cdot\mathbf{r})$.

Atom-field coupling

Rabi frequency

Atom-field Hamiltonian:

$$H_I = -\mathbf{d}\cdot\mathbf{E}_0\cos(\omega t + \varphi - \mathbf{k}\cdot\hat{\mathbf{r}})(\sigma_+ + \sigma_-)$$

$$H_I = \frac{\hbar\Omega}{2}\left(e^{i\omega t + i\varphi - i\mathbf{k}\cdot\hat{\mathbf{r}}} + e^{-i\omega t - i\varphi + i\mathbf{k}\cdot\hat{\mathbf{r}}}\right)(\sigma_+ + \sigma_-)$$

with definition of the Rabi frequency

$$\boxed{\Omega = -\frac{\mathbf{d}\cdot\mathbf{E}_0}{\hbar}}$$

In the case where both $\Delta = \omega - \omega_{eg}$ and Ω are much smaller than ω, Rotating wave approximation (RWA) applies and we can write (see later)

$$\boxed{H_I \simeq \frac{\hbar\Omega}{2}\left(e^{-i\omega t - i\varphi + i\mathbf{k}\cdot\hat{\mathbf{r}}}\sigma_+ + e^{i\omega t + i\varphi - i\mathbf{k}\cdot\hat{\mathbf{r}}}\sigma_-\right)}$$

Coherent coupling vs spontaneous decay

Coupling to the empty modes of the field

Fermi Golden rule applied between excited atom and empty modes of the field coupled by electric dipolar coupling, near the frequency $\omega \sim \omega_{eg}$

$\Gamma \propto |\langle g|W|e\rangle|^2 \propto d^2$

$$\Gamma = \frac{d^2 \omega_{eg}^3}{3\pi\hbar\varepsilon_0 c^3}$$

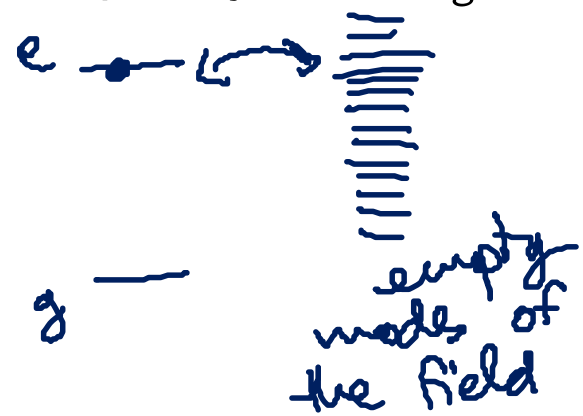

Γ: linewidth of the transition

Limit cases:

- $\Gamma \gg \Omega$: strong transition / short-lived state $|e\rangle$: evolution of the density matrix $\hat{\rho}$ to compute the light forces (OBE).
- $\Gamma \ll \Omega$: weak transition / long-lived state $|e\rangle$: hamiltonian evolution (Rabi oscillations) of quantum states $|\psi\rangle$ for quantum gates

Short-lived excited state and moving atom: Light forces

Classical atom motion

For a free two-level atom, classical external motion $(\mathbf{r}, \mathbf{v})$, interacting with a near resonant classical laser field

$$\mathbf{E}(\mathbf{r}, t) = \mathcal{E}_0 \mathbf{u}_x \cos(\omega t + \varphi - \mathbf{k} \cdot \mathbf{r})$$

on can derive light forces from the dipolar interation $-\hat{\mathbf{D}} \cdot \mathbf{E}(\mathbf{r}, t)$ and the optical Bloch equations (see e.g. CCT/DGO book).

laser

$\vec{k}, \omega$

$\bullet \rightarrow \hbar\vec{k}$

kick $\hbar\vec{k}$ when a photon is absorbed

$\Rightarrow$ Force $\sim \Gamma_{\text{scattering}} \hbar\vec{k}$

$$\Gamma_{\text{scattering}} \sim \frac{I/I_s}{\frac{I}{I_s} + 1 + 4\frac{\Delta^2}{\Gamma^2}}$$

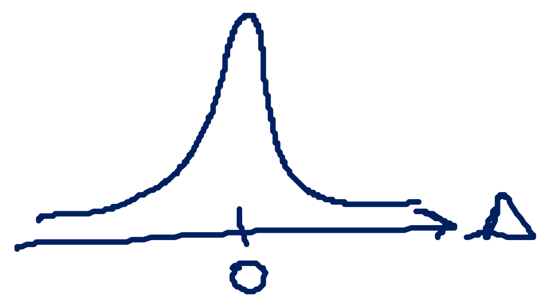

Short-lived excited state and moving atom: Light forces

Classical atom motion

For a free two-level atom, classical external motion $(\mathbf{r}, \mathbf{v})$, interacting with a near resonant classical laser field

$$\mathbf{E}(\mathbf{r}, t) = \mathcal{E}_0 \mathbf{u}_x \cos(\omega t + \varphi - \mathbf{k}\cdot\mathbf{r})$$

on can derive light forces from the dipolar interation $-\hat{\mathbf{D}}\cdot\mathbf{E}(\mathbf{r}, t)$ and the optical Bloch equations (see e.g. CCT/DGO book). Radiation pressure force in the direction of the laser due to **momentum conservation**, computed at **detuning** $\Delta = \omega - \omega_{eg} - \mathbf{k}\cdot\mathbf{v}$

$$\boxed{\mathbf{F}_{\rm pr}(\mathbf{v}) = \frac{\Gamma}{2}\frac{s_0}{1 + s_0 + 4\Delta^2/\Gamma^2}\hbar\mathbf{k}}$$

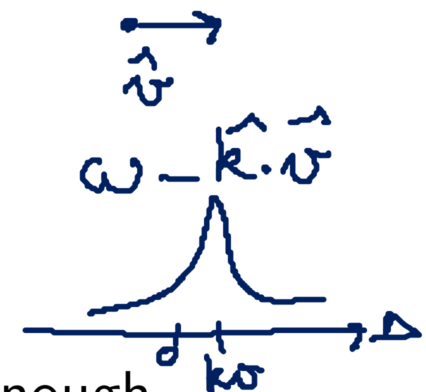

Γ: **linewidth** (inverse lifetime) of the excited state, large enough. With a red detuned laser beam, i.e. $\omega < \omega_{eg}$, the force is larger if $\mathbf{v}$ is **opposite** to the laser direction $\mathbf{k}$.

Laser cooling of the (classical) ion motion

(1) Doppler cooling

Trap of frequency ω_0. Two successive steps.
(1) Doppler cooling on a broad transition $\Gamma \gg \omega_0$ (Γ^{-1} lifetime of the electronic excited state) when the ion motion is still classical ($k_B T \gg \hbar\omega_0$). It makes use of the radiation pressure.
Two counter-propagating red detuned laser beams:

$\omega - \omega_{eg} < 0$

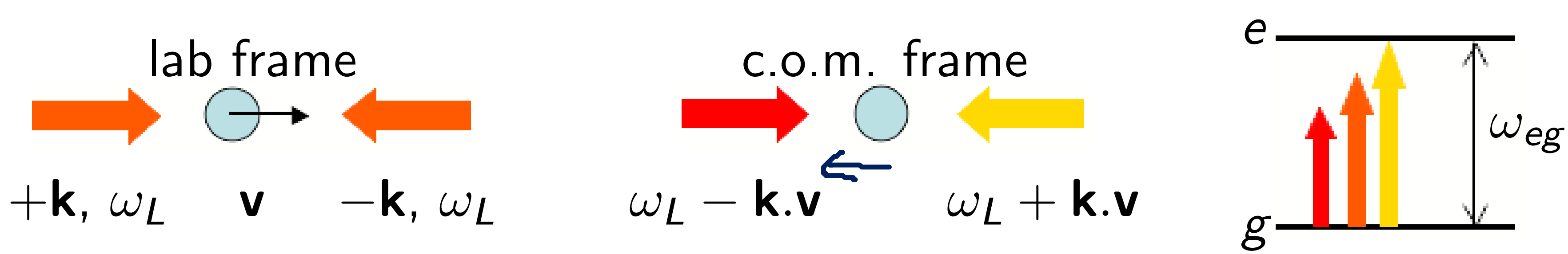

The force is larger when the apparent frequency is closer to resonance

$\Rightarrow$ net force against the atomic velocity.

Laser cooling of the (classical) ion motion

(1) Doppler cooling

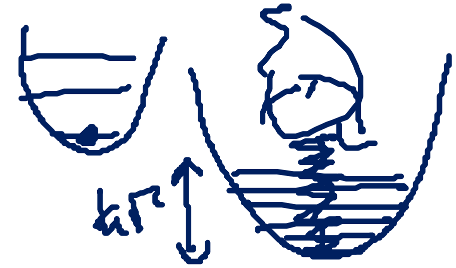

Trap of frequency ω_0. Two successive steps.
(1) Doppler cooling on a broad transition $\Gamma \gg \omega_0$ (Γ^{-1} lifetime of the electronic excited state) when the ion motion is still classical ($k_B T \gg \hbar\omega_0$). It makes use of the radiation pressure.

$\vec{v}$ $\vec{F}$

Two counter-propagating red detuned laser beams:

center-of-mass

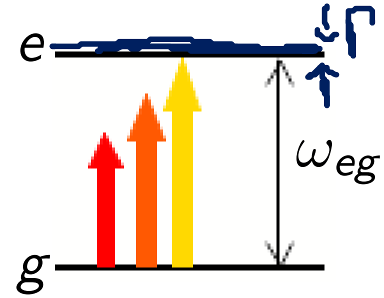

The force is larger when the apparent frequency is closer to resonance

$\Rightarrow$ net force against the atomic velocity.

$M\frac{d\vec{v}}{dt} + \alpha\vec{v} = 0$

At low velocity we get a friction force $\mathbf{F} = -\alpha\mathbf{v}$ with a friction coefficient $\alpha > 0$ for $\omega_L < \omega_{eg}$. Final temperature: $k_B T \sim \hbar\Gamma \gg \hbar\omega_0$.

$T \sim 100\ \mu K$

Laser cooling of the (quantum) ion motion

(2) Resolved sideband cooling

Recall: $$H_I \simeq \frac{\hbar\Omega}{2}\left(e^{-i\omega t - i\varphi + i\mathbf{k}\cdot\hat{\mathbf{r}}}\sigma_+ + e^{i\omega t + i\varphi - i\mathbf{k}\cdot\hat{\mathbf{r}}}\sigma_-\right)$$

1D $\hat{r} \longrightarrow \hat{x} = x_0(a + a^\dagger)$. $\quad \eta = k x_0 = \frac{2\pi x_0}{\lambda} \ll 1$

$$e^{-i\omega t - i\varphi}\, e^{ik\hat{x}} \qquad e^{ik\hat{x}} = e^{i\eta(a+a^\dagger)} \simeq 1 + i\eta(a + a^\dagger)$$

$$e^{ik\hat{x}}\sigma_+ \simeq \sigma_+ + i\eta\, a\sigma_+ + i\eta\, a^\dagger\sigma_+$$

$$H_I = H_c + H_{BSB} + H_{RSB} \qquad H_{BSB} = i\eta\frac{\hbar\Omega}{2}\left(e^{-\cdots}a^\dagger\sigma_+ + e^{\cdots}a\sigma_-\right)$$

$$H_c = \frac{\hbar\Omega}{2}\left(\cdots\sigma_+ + \cdots\sigma_-\right) \qquad H_{RSB} = i\eta\frac{\hbar\Omega}{2}\left(e^{\cdots}a\sigma_+ + e^{-\cdots}a^\dagger\sigma_-\right)$$

Laser cooling of the (quantum) ion motion

(2) Resolved sideband cooling

H_c carrier

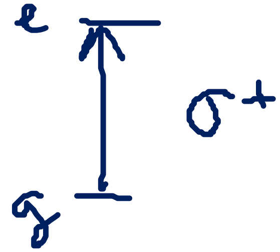

$\omega = \omega_{eg}$ does not change $|n\rangle$.

$$\frac{\hbar\Omega}{2}(\sigma_+ + \sigma_-)$$

H_{BSB} : blue sideband

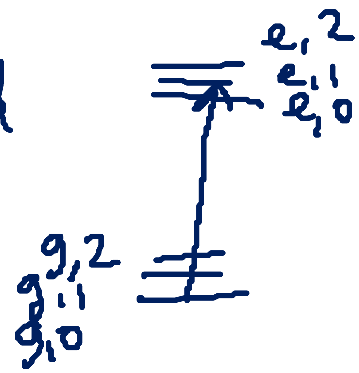

$$i\eta\frac{\hbar\Omega}{2}(a^\dagger\sigma_+ + a\sigma_-)$$

$g,n \longrightarrow e,n+1$

H_{RSB} : red sideband

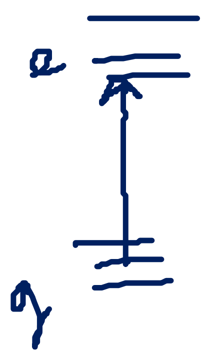

$g,n \longrightarrow e,n-1$

$$i\hbar\eta\frac{\Omega}{2}(a\sigma_+ + a^\dagger\sigma_-)$$

Laser cooling of the (quantum) ion motion

(2) Resolved sideband cooling

- To get to the ground state $n = 0$ of harmonic trap: use a narrow transition $\Gamma < \omega_0$.
- Transitions between vibrational states are now resolved. Coupling in the Lamb-Dicke regime $\eta = kx_0 \ll 1$:

  $$e^{ik\hat{x}}\sigma_+ = e^{i\eta(\hat{a}+\hat{a}^\dagger)}\sigma_+ \simeq \left[\mathbf{1} + \eta(\hat{a} + \hat{a}^\dagger)\right]\sigma_+$$

  carrier (σ_+) at ω_{eg}, red sideband ($\hat{a}\sigma_+$) at $\omega_{eg} - \omega_0$, blue sideband ($\hat{a}^\dagger\sigma_+$) at $\omega_{eg} + \omega_0$
- (1) Shine a laser on the $|g, n\rangle \to |e, n-1\rangle$ transition.
- (2) In the Lamb-Dicke regime, spontaneous emission back to $|g\rangle$ preserves the vibrational state $|n\rangle_{\text{ph}}$: $|e, n-1\rangle \to |g, n-1\rangle$.
- Energy $\hbar\omega_0$ lost at each cycle.
- Repeat until $|g, 0\rangle$ (uncoupled!) is reached.

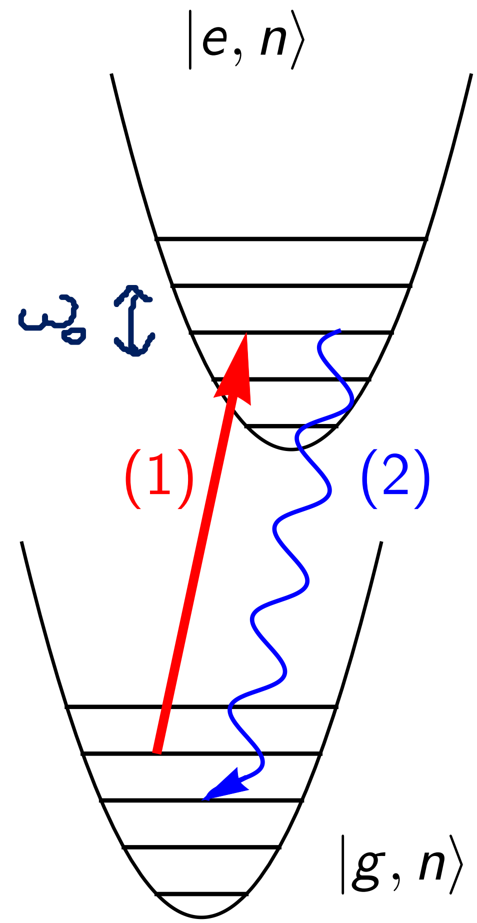

Resolved sideband cooling to the ground state

- spectrum after Doppler cooling: red sideband still visible
- spectrum after sideband cooling: only blue sideband remains, red sideband has disappeared
- In general, temperature can be estimated from the red/blue ratio $P_{\text{red}}/P_{\text{blue}} = \langle n \rangle / (1 + \langle n \rangle)$

$$\langle n \rangle = \frac{1}{e^{\hbar\omega_0/k_B T} - 1}$$

$$\Rightarrow \frac{P_{\text{red}}}{P_{\text{blue}}} = e^{-\hbar\omega_0/k_B T}$$

red sideband　　blue sideband

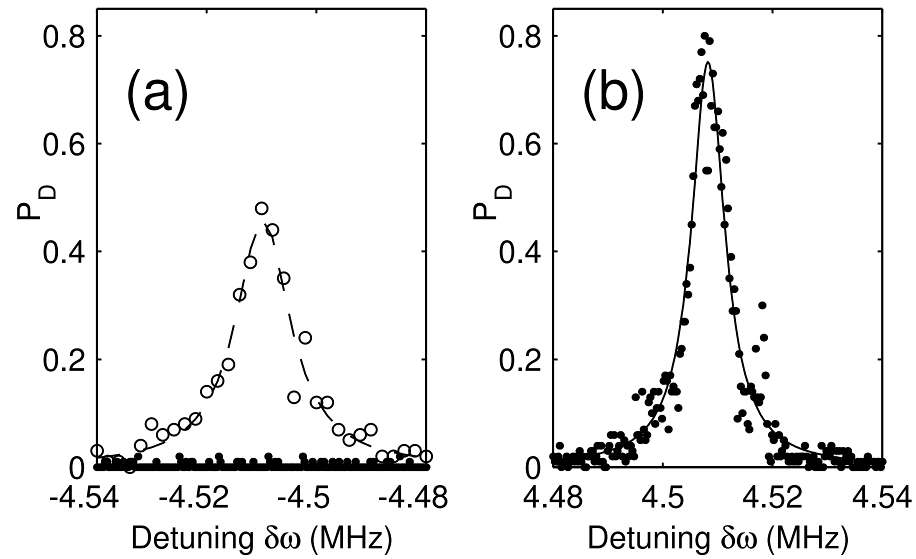

Cooling: time evolution of $\langle n \rangle$

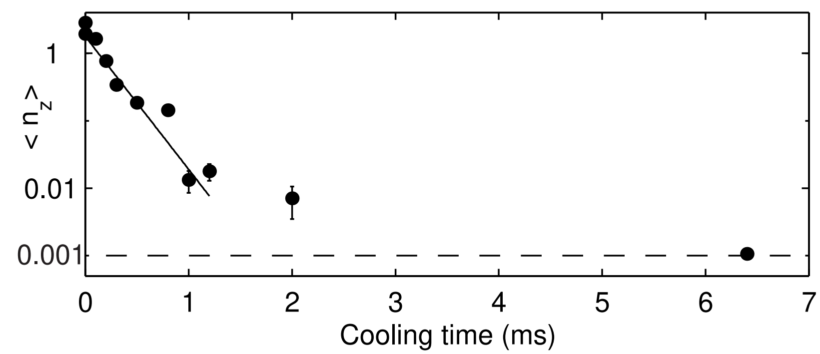

Fig. from Roos et al., PRL **83**, 4713

The qubit: a two-level system

The strong Doppler cooling transition is **not used** for the qubit (decoherence due to spontaneous decay of state $|e\rangle$).
Instead the two-level system used to define the qubit in ions can be of different nature:

- Zeeman qubit: between two Zeeman sublevels in the presence of a magnetic field ($\sim$ few MHz)
- Hyperfine qubit: between two hyperfine states ($\sim$ few GHz) driven by microwave or Raman transitions
- Fine structure qubit: between two states split by the fine structure ($\sim$ few THz)
- Optical qubit: between two stable electronic states, can be a 'clock transition' ($\sim$ few 100 ~~M~~THz)

In this lecture we will mostly describe optical qubits.

Typical level structure

Different kinds of qubits:

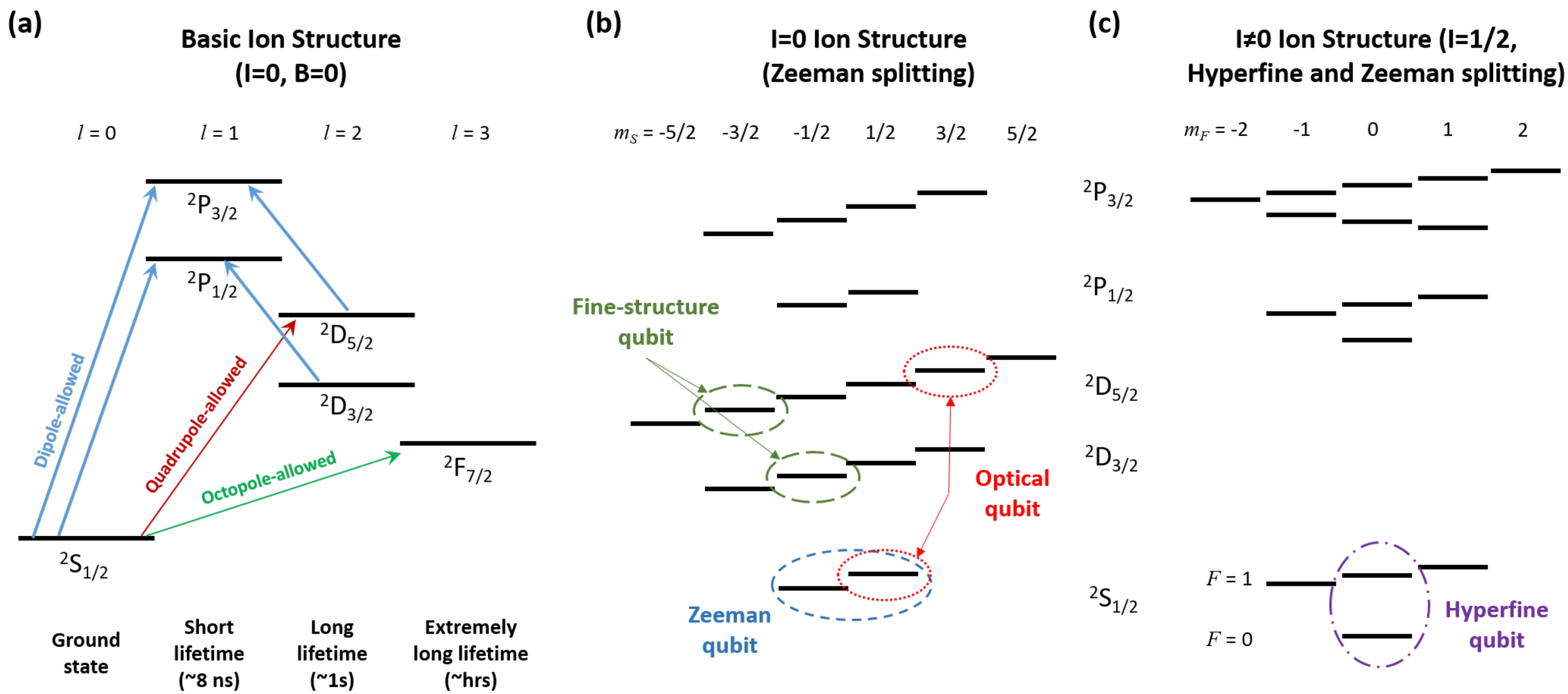

Figure from Bruzewicz et al.

Typical level structure: Optical qubit

Ions used for quantum computation as well as clocks are typically alkaline earth atoms (Be^+, Mg^+, Ca^+, Sr^+) or ytterbium Yb^+.

Optical qubit: two **long-lived states** $|0\rangle$ (ex: $D_{5/2}$) weekly coupled to the ground state $|1\rangle$ (ex: $S_{1/2}$)
Laser cooling and **detection**:
Short lived state $|e\rangle$ (ex: $P_{3/2}$), strongly coupled to ground state $|1\rangle$

$\begin{pmatrix} 1 & 0 \\ 0 & -1 \end{pmatrix}\begin{pmatrix} \; \\ \; \end{pmatrix}$ $\leftarrow 0$ $\leftarrow 1$

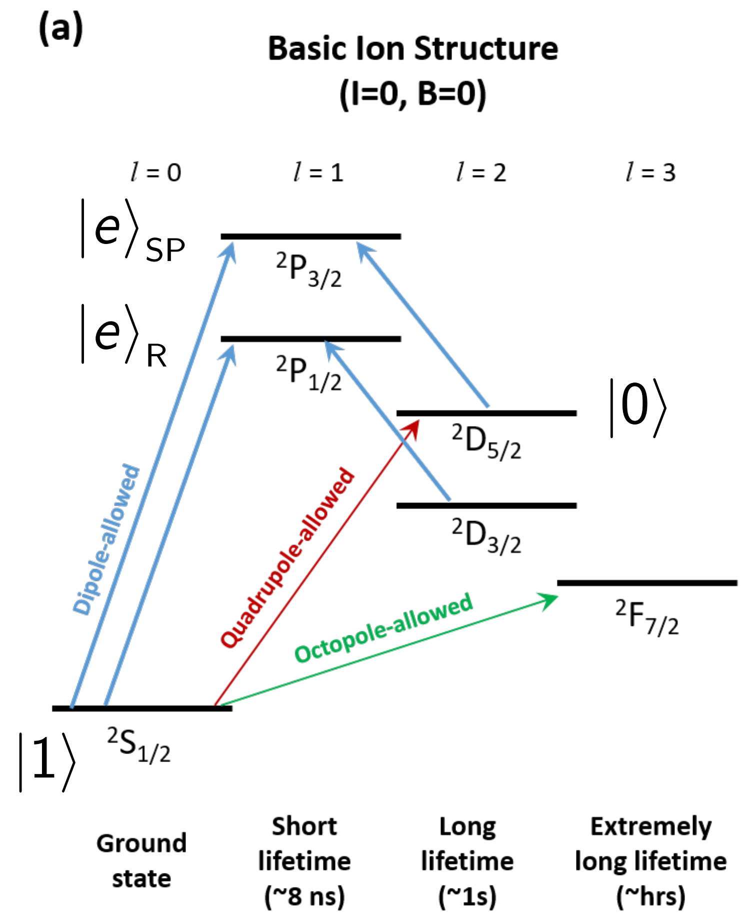

Figure from Bruzewicz et al.

Simplified level structure

The three operations performed on the ion state:

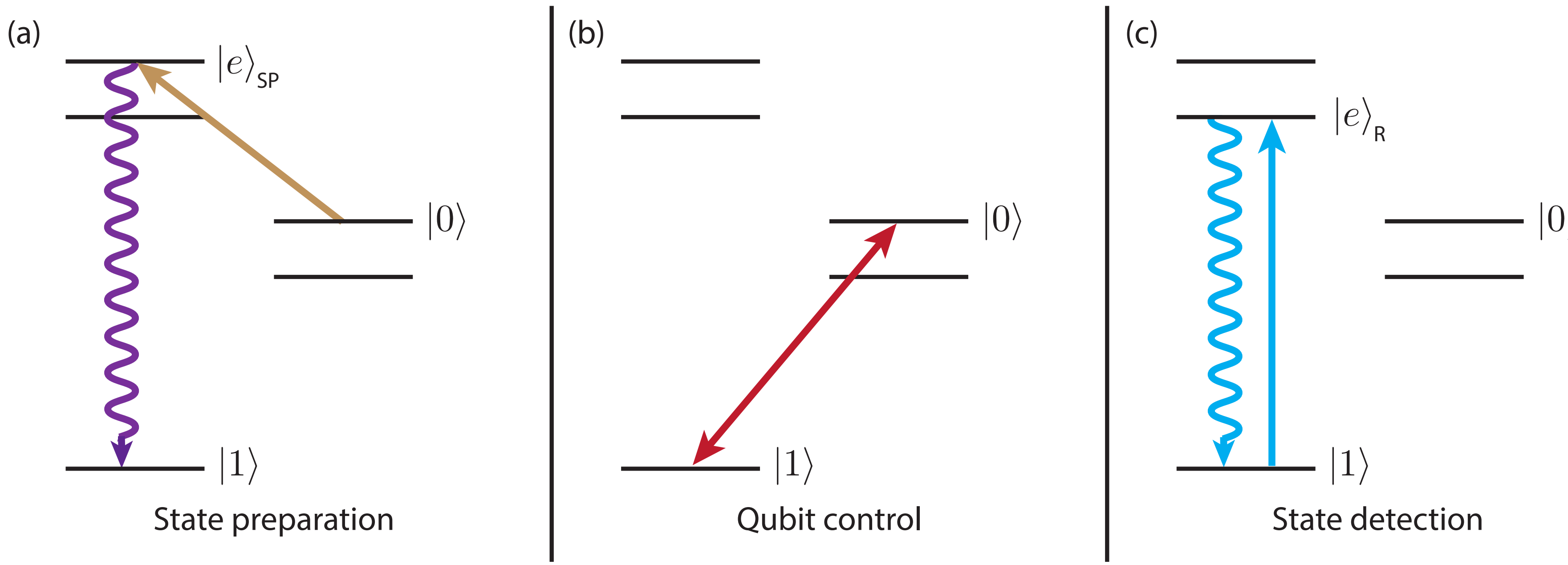

Figure from Bruzewicz et al.
$+$ for each **long-lived electronic state** $|0\rangle$ and $|1\rangle$, a ladder of phonon excitations $|n\rangle_{\text{ph}}$. Not relevant for $|e\rangle$ ($\Gamma \gg \omega_0$).

Qubit rotation (narrow line transition)

Carrier and sidebands

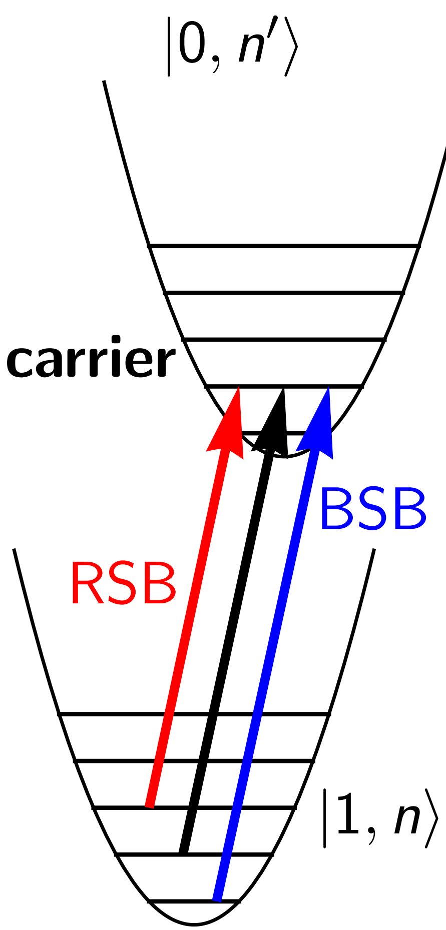

- Two states $|\uparrow\rangle \equiv |0\rangle$ and $|g\rangle \equiv |\downarrow\rangle \equiv |1\rangle$.
- Long lifetime $\Rightarrow$ no spontaneous decay, coherent (hamiltonian) evolution of the state.
- Coupling in the Lamb-Dicke regime $\eta = kx_0 \ll 1$:

$$e^{ik\hat{x}}\sigma_+ \simeq \left[\mathbf{1} + \eta(\hat{a} + \hat{a}^\dagger)\right]\sigma_+$$

- **carrier** (σ_+) at ω_{01}: $|1, n\rangle \leftrightarrow |0, n\rangle$
- red sideband $(\hat{a}\sigma_+)$ at $\omega_{01} - \omega_0$: $|1, n\rangle \leftrightarrow |0, n-1\rangle$
- blue sideband $(\hat{a}^\dagger\sigma_+)$ at $\omega_{01} + \omega_0$: $|1, n\rangle \leftrightarrow |0, n+1\rangle$

Let's describe in more detail the **carrier transition**, such that we can ignore the phonon state $|n\rangle_{\text{ph}}$.

Qubit rotation: Narrow line transition at carrier frequency

Atomic system seen as a spin

Two states $|\uparrow\rangle \equiv |0\rangle$ (or $|0_z\rangle$) and $|g\rangle \equiv |\downarrow\rangle \equiv |1\rangle$ (or $|1_z\rangle$).

Operator basis set: Pauli operators

$$\sigma_x = \begin{pmatrix} 0 & 1 \\ 1 & 0 \end{pmatrix} \qquad \sigma_y = \begin{pmatrix} 0 & -i \\ i & 0 \end{pmatrix} \qquad \sigma_z = \begin{pmatrix} 1 & 0 \\ 0 & -1 \end{pmatrix}$$

$$[\sigma_x, \sigma_y] = 2i\sigma_z \quad \text{and the other circular permutations}$$

Spin lowering and raising operators

$$\sigma_+ = |\uparrow\rangle\langle\downarrow| = |0\rangle\langle 1| = \frac{\sigma_x + i\sigma_y}{2} = \begin{pmatrix} 0 & 1 \\ 0 & 0 \end{pmatrix}$$

$$\sigma_- = |\downarrow\rangle\langle\uparrow| = |1\rangle\langle 0| = \sigma_+^\dagger = \frac{\sigma_x - i\sigma_y}{2} = \begin{pmatrix} 0 & 0 \\ 1 & 0 \end{pmatrix}$$

$$[\sigma_z, \sigma_\pm] = \pm 2\sigma_\pm$$

Arbitrary state of the two-level system

Most general observable $\sigma_{\mathbf{u}}$ with $\mathbf{u} = (\sin\theta\cos\phi, \sin\theta\sin\phi, \cos\theta)$

$$\sigma_{\mathbf{u}} = \sigma \cdot \mathbf{u} = \begin{pmatrix} \cos\theta & \sin\theta e^{-i\phi} \\ \sin\theta e^{i\phi} & -\cos\theta \end{pmatrix}.$$

$|0\rangle \equiv |0_z\rangle$

$|1\rangle \equiv |1_z\rangle$

Eigenvectors

$$|\uparrow_{\mathbf{u}}\rangle = |0_{\mathbf{u}}\rangle = \cos\frac{\theta}{2}|0\rangle + \sin\frac{\theta}{2}e^{i\phi}|1\rangle$$

$$|\downarrow_{\mathbf{u}}\rangle = |1_{\mathbf{u}}\rangle = -\sin\frac{\theta}{2}e^{-i\phi}|0\rangle + \cos\frac{\theta}{2}|1\rangle$$

Representation on the Bloch sphere

States $|0\rangle$, $|1\rangle$, $|0_x\rangle$, $|0_y\rangle$, $|0_{\mathbf{u}}\rangle$:

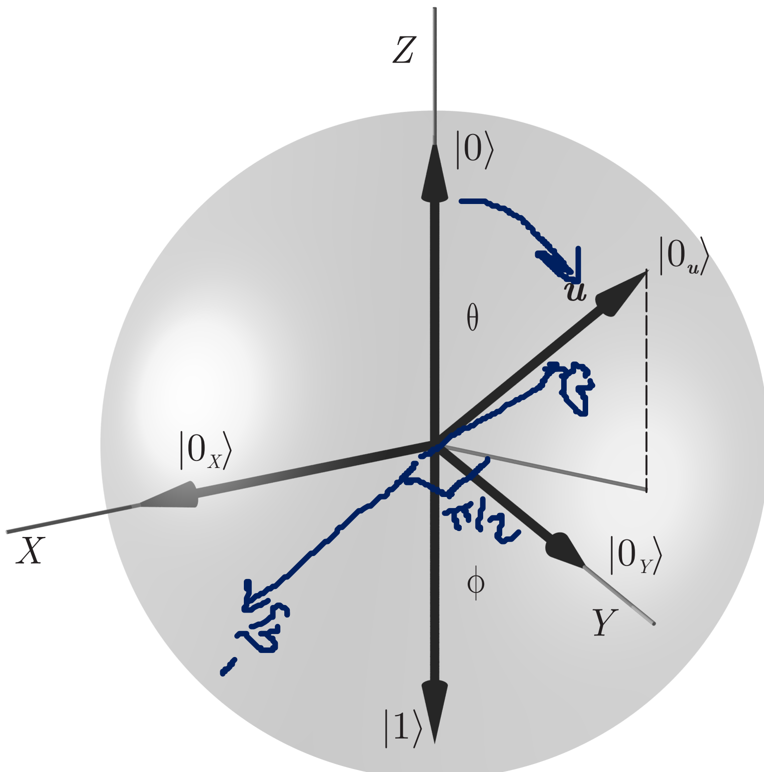

State rotation $R_{\mathbf{v}}(\alpha)$ by an angle α around the axis defined by $\mathbf{v}$:

$$R_{\mathbf{v}}(\alpha) = e^{-i(\alpha/2)\sigma_{\mathbf{v}}} = \cos\frac{\alpha}{2}\mathbb{1} - i\sin\frac{\alpha}{2}\sigma_{\mathbf{v}}$$

N.B. $R_{\mathbf{v}}(2\pi) = -\mathbb{1}$

$|0_{\mathbf{u}}\rangle$, $|1_{\mathbf{u}}\rangle$ obtained by a rotation of $|0\rangle$, $|1\rangle$ of angle θ around the axis $\mathbf{v} = (-\sin\phi, \cos\phi, 0)$.

Rotation of states on the Bloch sphere

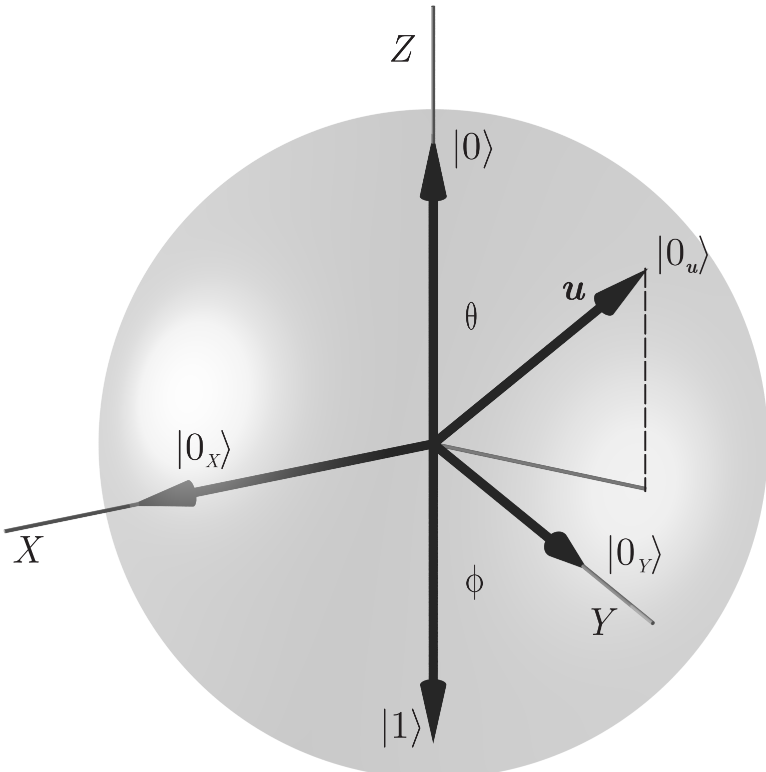

Around $\mathbf{u}_z$: $R_z(\alpha) = \begin{pmatrix} e^{-i\alpha/2} & 0 \\ 0 & e^{i\alpha/2} \end{pmatrix}$

phase gate Z: $R_z(\pi) = -i\sigma_z = -i\begin{pmatrix} 1 & 0 \\ 0 & -1 \end{pmatrix}$

Around $\mathbf{u}_x$: $R_x(\alpha) = \begin{pmatrix} \cos\frac{\alpha}{2} & -i\sin\frac{\alpha}{2} \\ -i\sin\frac{\alpha}{2} & \cos\frac{\alpha}{2} \end{pmatrix}$

spin flip X: $R_x(\pi) = -i\sigma_x = -i\begin{pmatrix} 0 & 1 \\ 1 & 0 \end{pmatrix}$

Around $\mathbf{u}_y$: $R_y(\alpha) = \begin{pmatrix} \cos\frac{\alpha}{2} & -\sin\frac{\alpha}{2} \\ \sin\frac{\alpha}{2} & \cos\frac{\alpha}{2} \end{pmatrix}$

Hadamard gate H:

$R_y(\frac{\pi}{2})\,|0\rangle = \frac{1}{\sqrt{2}}(|0\rangle + |1\rangle) = |0_x\rangle \qquad R_y(\frac{\pi}{2})\,|1\rangle = \frac{1}{\sqrt{2}}(-|0\rangle + |1\rangle) = |1_x\rangle$

Laser coupling at $\omega \simeq \omega_{01}$

Hamiltonian ignoring external motion (carrier), detuning $\Delta = \omega - \omega_{01}$:

$$H = \frac{\hbar\omega_{01}}{2}\sigma_z + \frac{\hbar\Omega}{2}\left(e^{i\omega t + i\varphi} + e^{-i\omega t - \varphi}\right)(\sigma_+ + \sigma_-) = H_0' - \frac{\hbar\Delta}{2}\sigma_z + H_I$$

Interaction representation with respect to $H_0' = \hbar\omega\sigma_z/2$ inducing a spin precession at the field frequency ω.
Hamiltonian for $|\tilde\psi\rangle = U_0'^{\dagger}\,|\psi\rangle$ (hence $|\psi\rangle = U_0'|\tilde\psi\rangle$) with
$U_0'^{\dagger} = \exp(iH_0't/\hbar)$ i.e. $U_0' = \exp(-iH_0't/\hbar) = e^{-i\frac{\omega t}{2}\sigma_z} = R_z(\omega t)$:

$$i\hbar\partial_t|\tilde\psi\rangle = i\hbar\,\partial_t U_0'^{\dagger}|\psi\rangle + U_0'^{\dagger}\, i\hbar\partial_t|\psi\rangle = \cancel{-H_0'U_0'^{\dagger}|\psi\rangle} + U_0'^{\dagger}\left(\cancel{H_0'} - \frac{\hbar\Delta}{2}\sigma_z + H_I\right)|\psi\rangle$$

$$H_0'U_0'^{\dagger} = U_0'^{\dagger}H_0' \qquad = U_0'^{\dagger}\left(-\frac{\hbar\Delta}{2}\sigma_z + H_I\right)U_0'|\tilde\psi\rangle$$

$$i\hbar\partial_t|\tilde\psi\rangle = \tilde H|\tilde\psi\rangle \text{ where } \tilde H = U_0'^{\dagger}\left(-\frac{\hbar\Delta}{2}\sigma_z + H_I\right)U_0'$$

$$\tilde\sigma_\pm = U_0'^{\dagger}\sigma_\pm U_0' \qquad \tilde\sigma_\pm|1\rangle = e^{i\frac{\omega t}{2}\sigma_z}\sigma_+ e^{-i\frac{\omega t}{2}\sigma_z}|1\rangle = e^{i\frac{\omega t}{2}}e^{i\frac{\omega t}{2}}|0\rangle$$

Laser coupling at $\omega \simeq \omega_{01}$

Hamiltonian ignoring external motion (carrier), detuning $\Delta = \omega - \omega_{01}$:

$$H = \frac{\hbar\omega_{01}}{2}\sigma_z + \frac{\hbar\Omega}{2}\left(e^{i\omega t + i\varphi} + e^{-i\omega t - \varphi}\right)(\sigma_+ + \sigma_-) = H_0' - \frac{\hbar\Delta}{2}\sigma_z + H_I$$

Interaction representation with respect to $H_0' = \hbar\omega\sigma_z/2$ inducing a spin precession at the field frequency ω.

Hamiltonian for $|\tilde{\psi}\rangle = U_0'^{\dagger}|\psi\rangle$ with $U_0' = e^{-iH_0't/\hbar} = e^{-i\frac{\omega t}{2}\sigma_z} = R_z(\omega t)$:

$$\widetilde{H} = U_0'^{\dagger}\left(-\frac{\hbar\Delta}{2}\sigma_z + H_I\right)U_0'$$

σ_z part of H_0 unchanged (commutes with the evolution operator) but

$$\widetilde{\sigma}_\pm = U'^{\dagger}_0\sigma_\pm U'_0 = e^{i\frac{\omega t}{2}\sigma_z}\sigma_\pm e^{-i\frac{\omega t}{2}\sigma_z} = e^{\pm i\omega t}\sigma_\pm.$$

Spin rotation at $\omega \simeq \omega_{01}$

Rabi precession

$$\widetilde{H} = -\frac{\hbar\Delta}{2}\sigma_z + \frac{\hbar\Omega}{2}\left(e^{-i(\omega t+\varphi)} + e^{i(\omega t+\varphi)}\right)\left(e^{i\omega t}\sigma_+ + e^{-i\omega t}\sigma_-\right)$$

Two rapidly oscillating terms, and two constant ones.

Rotating wave approximation (RWA): neglect terms oscillating rapidly in $\widetilde{H}$

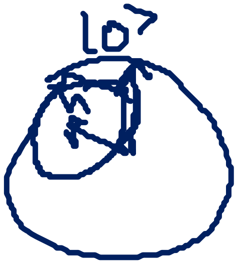

$$\begin{aligned}\widetilde{H} &= -\frac{\hbar\Delta}{2}\sigma_z + \frac{\hbar\Omega}{2}\left(\sigma_+ e^{-i\varphi} + \sigma_- e^{i\varphi}\right)\\ &= -\frac{\hbar\Delta}{2}\sigma_z + \frac{\hbar\Omega}{2}\left(\sigma_x\cos\varphi + \sigma_y\sin\varphi\right) = \frac{\hbar\Omega'}{2}\sigma_{\mathbf{n}}\end{aligned}$$

$\cos\theta = -\frac{\Delta}{\Omega'}$

$\sin\theta = \frac{\Omega}{\Omega'}$

with $\mathbf{n} = \dfrac{-\Delta\mathbf{u}_z + \Omega\cos\varphi\,\mathbf{u}_x + \Omega\sin\varphi\,\mathbf{u}_y}{\Omega'}$ and $\Omega' = \sqrt{\Omega^2+\Delta^2}$.

Hence, evolution operator $U(t) = e^{-i\frac{\Omega' t}{2}\sigma_{\mathbf{n}}} = R_{\mathbf{n}}(\Omega' t)$. Spin rotation!

To flip the spin completely, $\mathbf{n}$ should be in the horizontal plane $\Rightarrow \Delta = 0$.

Spin rotation at $\omega \simeq \omega_{01}$

Rabi precession

$$\widetilde{H} = \frac{\hbar\Omega'}{2}\sigma_{\mathbf{n}} \qquad \text{where} \qquad \Omega' = \sqrt{\Omega^2 + \Delta^2}$$

$$\mathbf{n} = \cos\theta\,\mathbf{u}_z + \sin\theta(\cos\varphi\,\mathbf{u}_x + \sin\varphi\,\mathbf{u}_y)$$

with $\cos\theta = -\Delta/\Omega'$ and $\sin\theta = \Omega/\Omega'$.

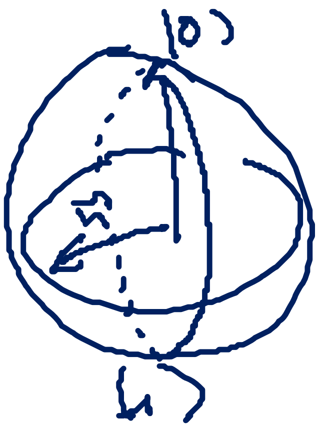

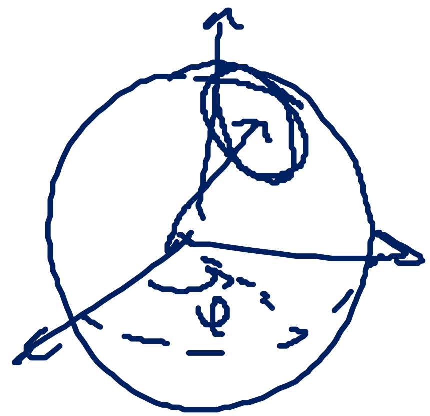

Resonant case $\Delta = 0$: Spin rotation at $\omega = \omega_{01}$

Rabi precession

$\Omega' = \Omega = \sqrt{\cancel{\Delta^2} + \Omega^2}$

Resonant case $\Delta = 0$: rotation around an axis in the equatorial plane $\mathbf{n} = \cos\varphi\,\mathbf{u}_x + \sin\varphi\,\mathbf{u}_y$. Choosing $|g\rangle = |1\rangle$ as the initial state

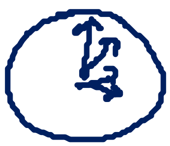

$$|\tilde{\psi}(t)\rangle = -i\,e^{-i\varphi}\sin\frac{\Omega t}{2}\,|0\rangle + \cos\frac{\Omega t}{2}\,|1\rangle$$

$$p_0(t) = \frac{1-\cos(\Omega t)}{2}$$

Rabi oscillation at frequency Ω.

More generally, evolution operator for $|\tilde{\psi}\rangle$:

$$U(t) = \begin{pmatrix} \cos\frac{\Omega t}{2} & -ie^{-i\varphi}\sin\frac{\Omega t}{2} \\ -ie^{i\varphi}\sin\frac{\Omega t}{2} & \cos\frac{\Omega t}{2} \end{pmatrix}$$

Resonant case $\Delta = 0$: Spin rotation at $\omega = \omega_{01}$

Rabi precession

Some particular choices of pulse duration:

- '$\pi/2$ pulse', i.e. $t = \pi/2\Omega$. Evolution operator

$$R_{\mathbf{n}}(\pi/2) = \frac{1}{\sqrt{2}}(\mathbb{1} - i\sigma_{\mathbf{n}}) = \frac{1}{\sqrt{2}}\begin{pmatrix} 1 & -ie^{-i\varphi} \\ -ie^{i\varphi} & 1 \end{pmatrix}$$

Recover Hadamard gate for $\varphi = \pi/2$: $\left\{\begin{array}{ccc} |0\rangle & \longrightarrow & \frac{1}{\sqrt{2}}(|0\rangle + |1\rangle) \\ |1\rangle & \longrightarrow & \frac{1}{\sqrt{2}}(-|0\rangle + |1\rangle) \end{array}\right.$

- 'π-pulse': $\Omega t = \pi$ with $\varphi = 0$. $R_x(\pi) = -i\sigma_x \Rightarrow$ Spin flip X-gate
- '2π pulse': $\Omega t = 2\pi$ global $-$ sign associated to a 2π rotation of a spin-1/2.

N.B. The Z-gate (π-rotation around Z, corresponding to $|\Delta| \gg \Omega$) is rather obtained by shifting the laser phase φ by π before next pulse.

Qubit rotation: Narrow line transition at sideband frequencies

Near a sideband transition, the two coupled states have different phonon excitations.

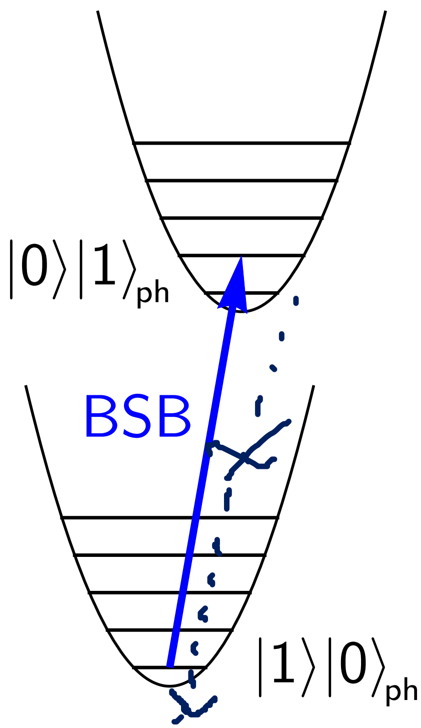

- Blue sideband: in the interaction picture and within RWA, coupling $\eta\Omega\sqrt{n+1}$

$$H_I = \frac{\hbar\eta\Omega}{2}\left(\hat{a}^\dagger\sigma_+ e^{-i\varphi} + \hat{a}\sigma_- e^{i\varphi}\right)$$

- Couples state $|1\rangle|0\rangle_{\mathrm{ph}}$ with $|0\rangle|1\rangle_{\mathrm{ph}}$. X-gate, Z-gate, Hadamard H-gate possible between these states. Example of $\pi/2$ pulse:

$$\begin{aligned} |0\rangle\,|1\rangle_{\mathrm{ph}} &\longrightarrow \frac{1}{\sqrt{2}}\left(|0\rangle\,|1\rangle_{\mathrm{ph}} + |1\rangle\,|0\rangle_{\mathrm{ph}}\right) \\ |1\rangle\,|0\rangle_{\mathrm{ph}} &\longrightarrow \frac{1}{\sqrt{2}}\left(-\,|0\rangle\,|1\rangle_{\mathrm{ph}} + |1\rangle\,|0\rangle_{\mathrm{ph}}\right) \end{aligned}$$

- BSB does nothing on $|0\rangle|0\rangle_{\mathrm{ph}}$ state!

Qubit rotation: Narrow line transition at sideband frequencies

Near a sideband transition, the two coupled states have different phonon excitations.

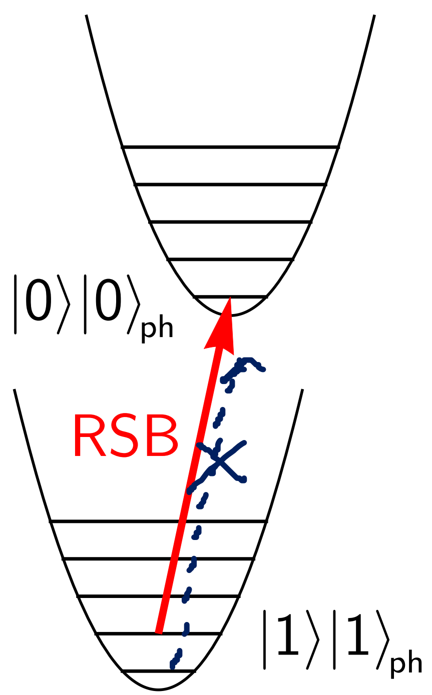

- Red sideband: in the interaction picture and within RWA, coupling $\eta\Omega\sqrt{n+1}$

$$H_I = \frac{\hbar\eta\Omega}{2}\left(\hat{a}\sigma_+ e^{-i\varphi} + \hat{a}^\dagger\sigma_- e^{i\varphi}\right)$$

- Couples state $|1\rangle|1\rangle_{\text{ph}}$ with $|0\rangle|0\rangle_{\text{ph}}$. X-gate, Z-gate, Hadamard H-gate possible between these states. Example of $\pi/2$ pulse:

$$|0\rangle\,|0\rangle_{\text{ph}} \longrightarrow \frac{1}{\sqrt{2}}\left(|0\rangle\,|0\rangle_{\text{ph}} + |1\rangle\,|1\rangle_{\text{ph}}\right)$$
$$|1\rangle\,|1\rangle_{\text{ph}} \longrightarrow \frac{1}{\sqrt{2}}\left(-\,|0\rangle\,|0\rangle_{\text{ph}} + |1\rangle\,|1\rangle_{\text{ph}}\right)$$

- RSB does nothing on $|1\rangle|0\rangle_{\text{ph}}$ state!

Qubit rotation: Experimental results

Carrier Rabi oscillations and blue sideband Rabi oscillations for a Ca^+ ion: different timescales. $S_{1/2} \to D_{5/2}$ line at 729 nm. Innsbruck group.

carrier
$2\pi/\Omega = 11\ \mu s$

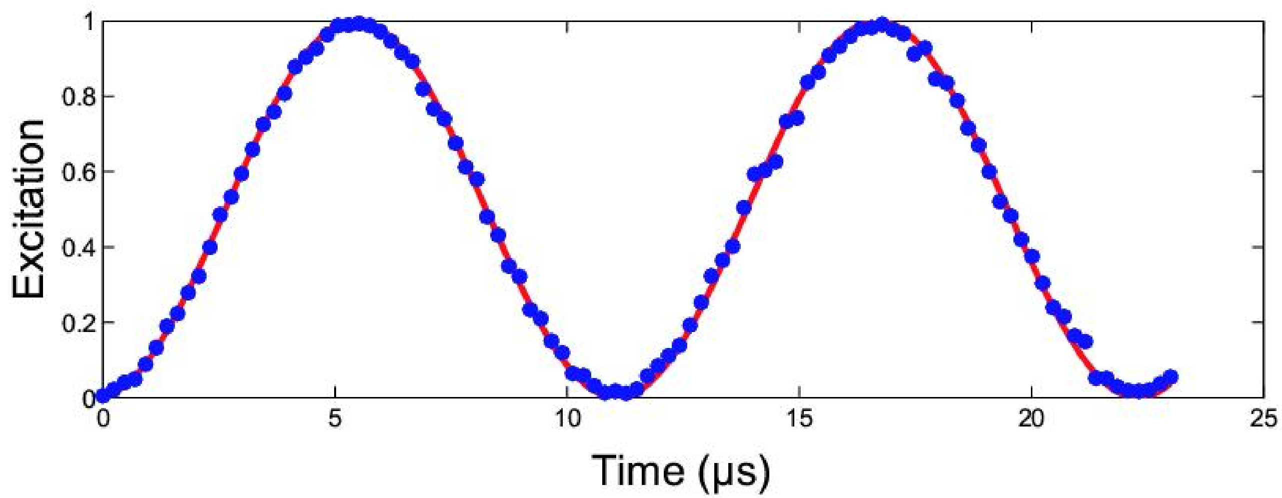

BSB
$2\pi/(\eta\Omega\sqrt{n+1}) = 270\ \mu s$

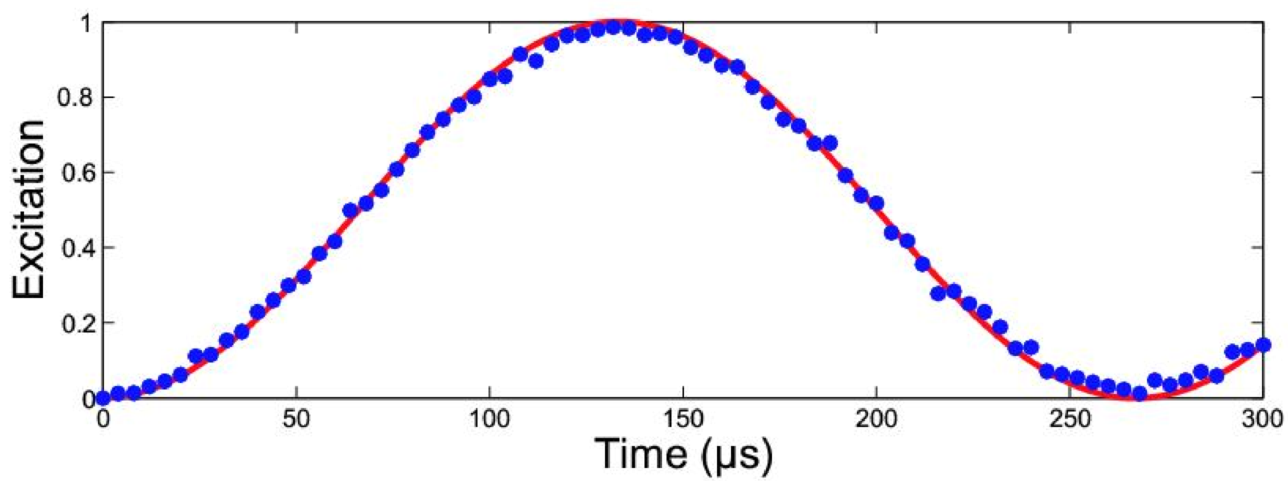

Detection of the qubit state (strong transition)

Electron shelving method

$|1\rangle$ strongly coupled to the excited state $|e\rangle$ (e.g. Doppler cooling transition). Photons scattering when driving the $|1\rangle \to |e\rangle$ transition. $|1\rangle$ is the **bright state** while the metastable $|0\rangle$ state remains **dark**.

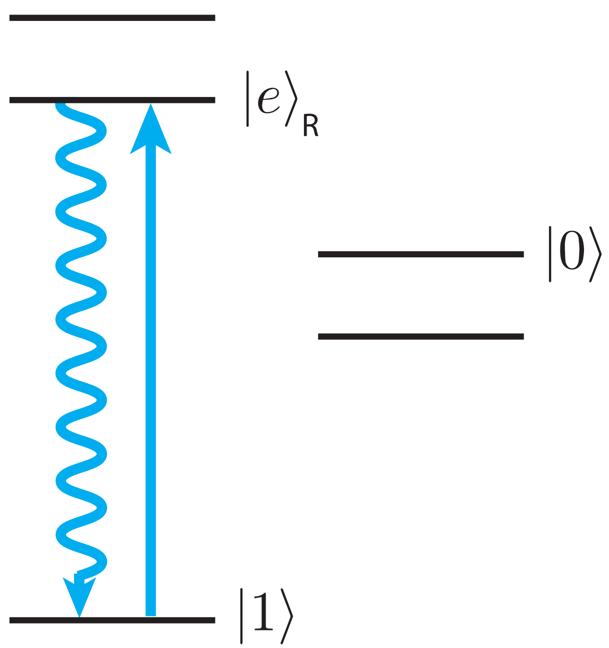

State detection

Fluorescence signal

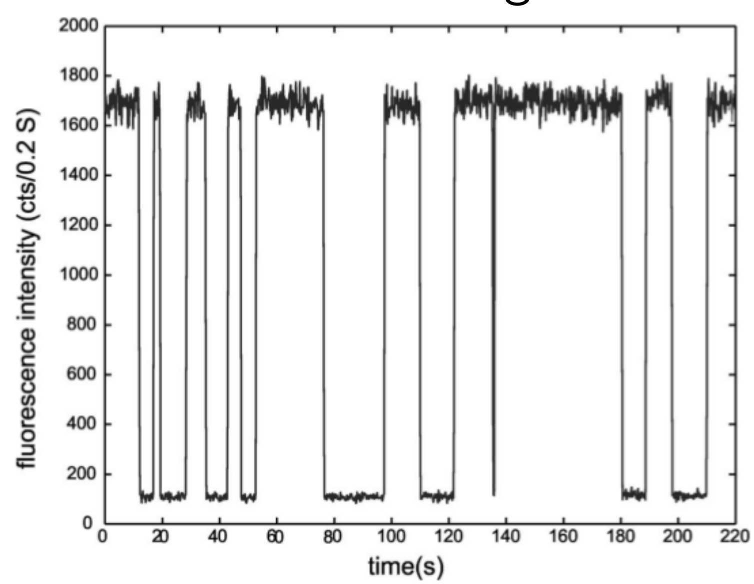

Observation of quantum jumps

Joint detection of the qubit and phonon state

Method valid for $n = 0, 1$

How to detect the state $|x\rangle|n\rangle_{\text{ph}}$? Repeat two kinds of measurements:

1. Search for $|0\rangle|n\rangle_{\text{ph}}$:

state	fluo	after BSB-π	fluo	signature
$\|0\rangle\|0\rangle_{\text{ph}}$	**dark**	$\|0\rangle\|0\rangle_{\text{ph}}$	**dark**	**DD**
$\|0\rangle\|1\rangle_{\text{ph}}$	**dark**	$\|1\rangle\|0\rangle_{\text{ph}}$	**bright**	**DB**
$\|1\rangle\|n\rangle_{\text{ph}}$	**bright**	-	-	**B**$\varnothing$

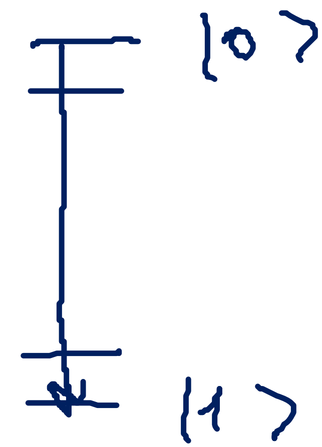

2. Search for $|1\rangle|n\rangle_{\text{ph}}$:

state	after **carrier**-π	fluo	after BSB-π	fluo	signature
$\|0\rangle\|0\rangle_{\text{ph}}$	$\|1\rangle\|0\rangle_{\text{ph}}$	**bright**	-	-	**B**$\varnothing$
$\|0\rangle\|1\rangle_{\text{ph}}$	$\|1\rangle\|1\rangle_{\text{ph}}$	**bright**	-	-	**B**$\varnothing$
$\|1\rangle\|0\rangle_{\text{ph}}$	$\|0\rangle\|0\rangle_{\text{ph}}$	**dark**	$\|0\rangle\|0\rangle_{\text{ph}}$	**dark**	**DD**
$\|1\rangle\|1\rangle_{\text{ph}}$	$\|0\rangle\|1\rangle_{\text{ph}}$	**dark**	$\|1\rangle\|0\rangle_{\text{ph}}$	**bright**	**DB**

Joint detection of the qubit and phonon state

Experimental results: Truth table

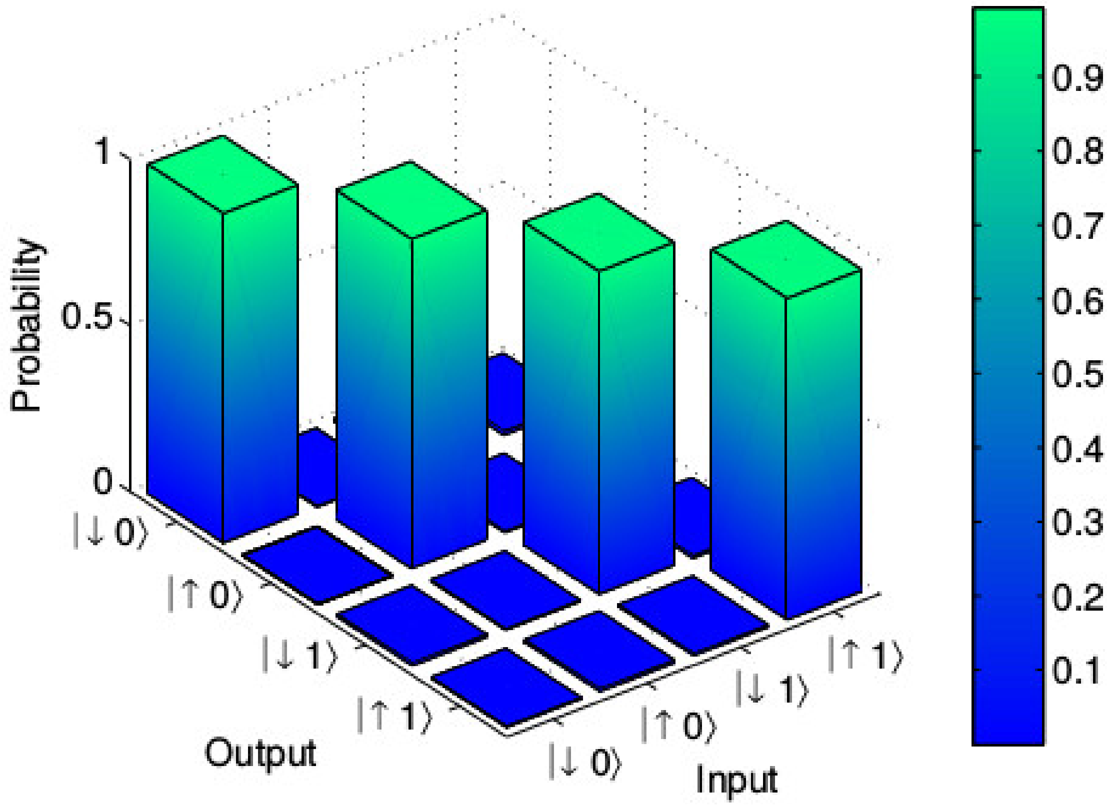

$$\begin{pmatrix} 99.0 & 0.3 & 1.0 & 1.2 \\ 0.0 & 99.2 & 0.4 & 1.0 \\ 0.8 & 0.3 & 97.2 & 0.8 \\ 0.3 & 0.8 & 0.5 & 96.7 \end{pmatrix}$$

with trapped, $^{88}Sr^{+}$, from J. Łabaziewicz PhD thesis (MIT, 2008)

Effect of a carrier-π pulse

Coupling: $\Omega(\sigma_+ + \sigma_-) \Rightarrow \pi$-pulse for $\Omega t = \pi$

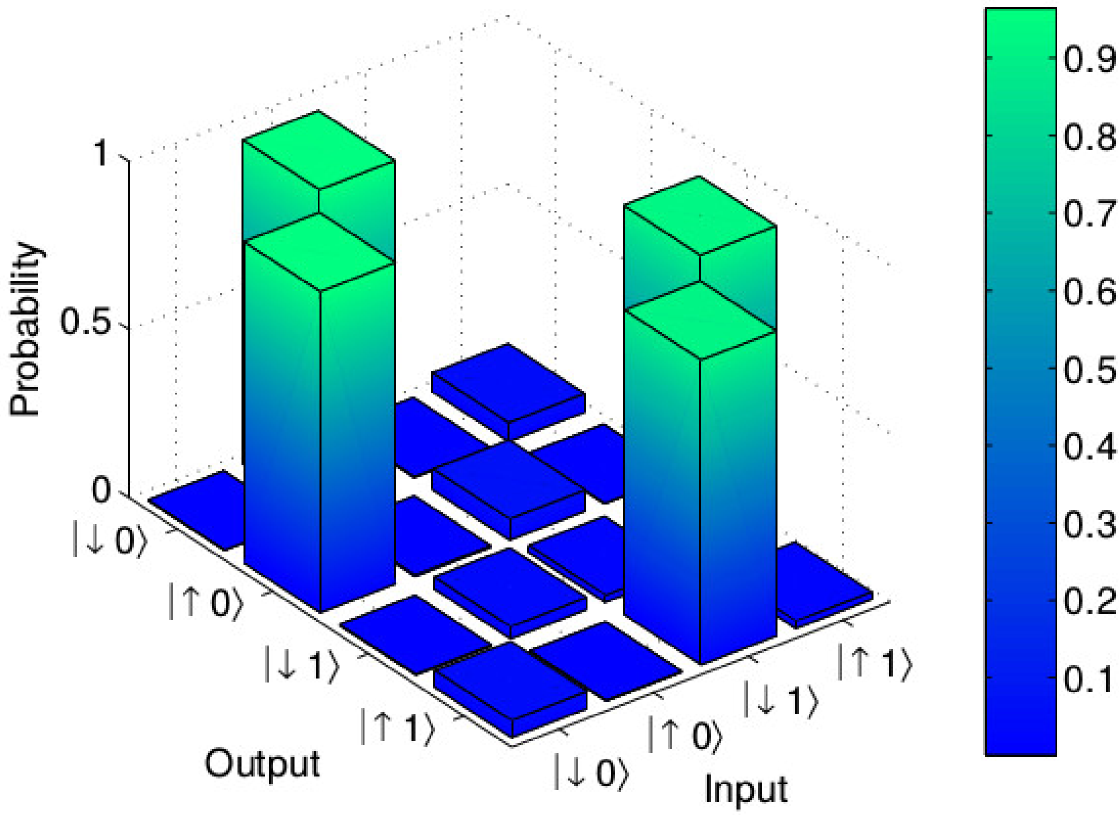

$$|1\rangle\,|0\rangle_{\text{ph}} \leftrightarrow |0\rangle\,|0\rangle_{\text{ph}}$$

$$|1\rangle\,|1\rangle_{\text{ph}} \leftrightarrow |0\rangle\,|1\rangle_{\text{ph}}$$

$$\begin{pmatrix} 0.1 & 96.4 & 0.3 & 5.5 \\ 95.4 & 0.4 & 6.2 & 0.1 \\ 0.2 & 3.5 & 2.1 & 92.4 \\ 5.0 & 0.1 & 90.5 & 2.1 \end{pmatrix}$$

with trapped, $^{88}\text{Sr}^+$, from J. Łabaziewicz PhD thesis (MIT, 2008)

Effect of a BSB-π pulse

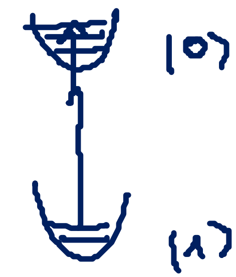

Coupling: $\Omega(\hat{a}^\dagger\sigma_+ + \hat{a}\sigma_-)$ does nothing on $|0\rangle|0\rangle_{\text{ph}}$ state

$\Omega a^\dagger\,|0\rangle_{\text{ph}} = \Omega\,|1\rangle_{\text{ph}} \Rightarrow \pi$-pulse on $|1\rangle\,|0\rangle_{\text{ph}} \leftrightarrow |0\rangle\,|1\rangle_{\text{ph}}$ for $\Omega t = \pi$

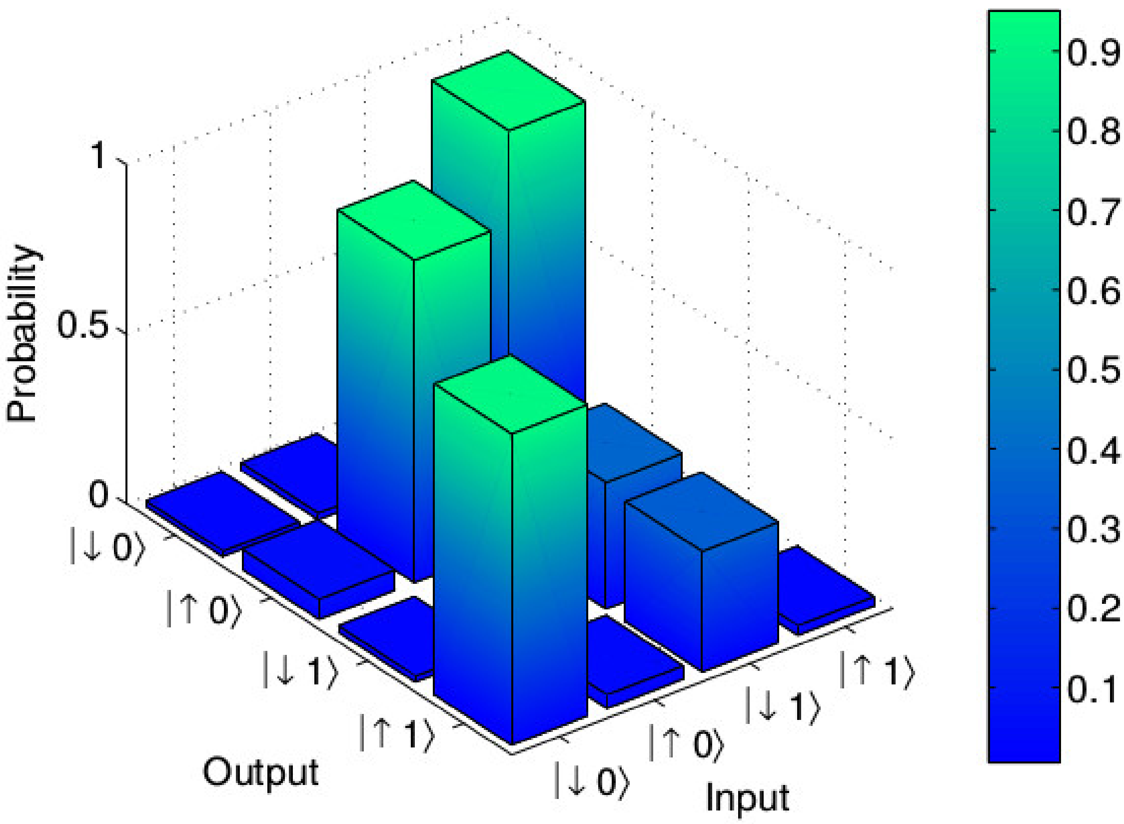

And for $|1\rangle\,|1\rangle_{\text{ph}} \rightarrow |0\rangle\,|2\rangle_{\text{ph}}$?

Effect of a BSB-π pulse

$a^\dagger|0\rangle = |1\rangle$

$\Omega \to \Omega$

$1\,1 \longrightarrow 0\,2$

$a^\dagger|1\rangle = \sqrt{2}\,|2\rangle$

$\Omega \to \sqrt{2}\,\Omega$

Coupling: $\Omega(\hat{a}^\dagger\sigma_+ + \hat{a}\sigma_-)$ does nothing on $|0\rangle|0\rangle_{\text{ph}}$ state

$\Omega a^\dagger\,|0\rangle_{\text{ph}} = \Omega\,|1\rangle_{\text{ph}} \Rightarrow \pi$-pulse on $|1\rangle\,|0\rangle_{\text{ph}} \leftrightarrow |0\rangle\,|1\rangle_{\text{ph}}$ for $\Omega t = \pi$

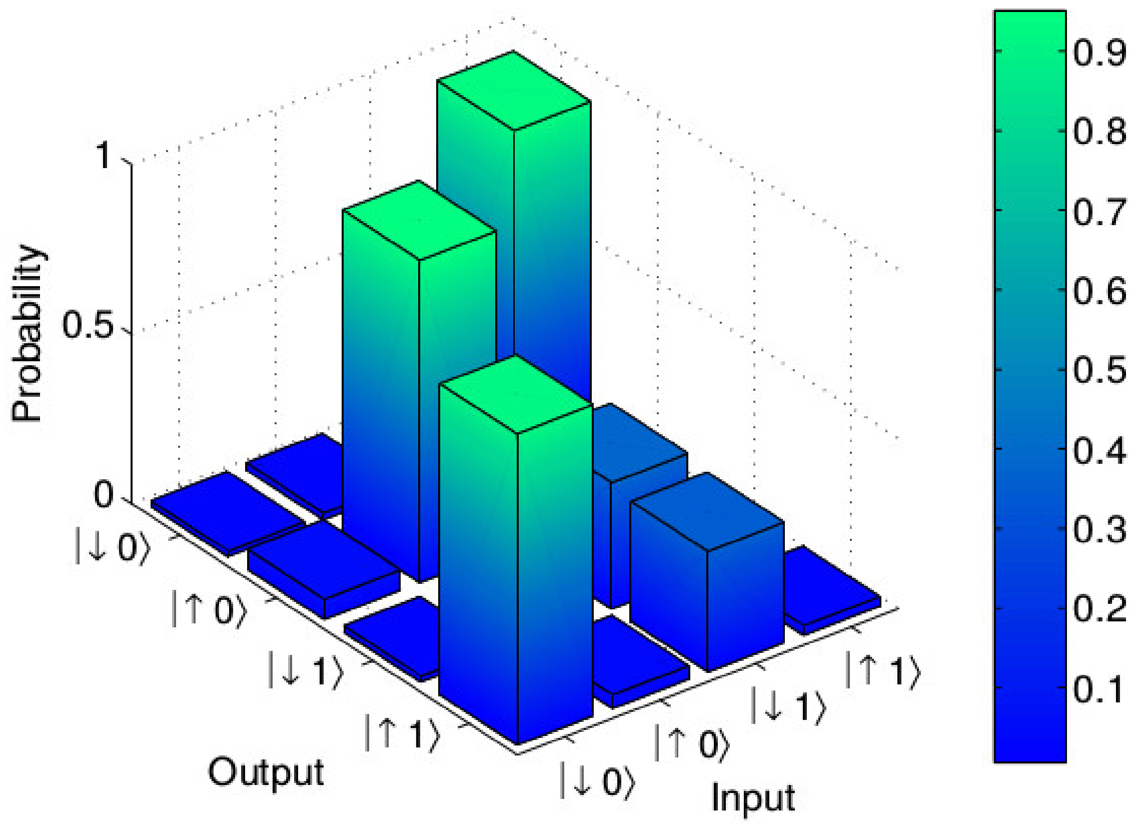

And for $|1\rangle\,|1\rangle_{\text{ph}} \to |0\rangle\,|2\rangle_{\text{ph}}$?

$\Omega a^\dagger\,|1\rangle_{\text{ph}} = \Omega\sqrt{2}\,|2\rangle_{\text{ph}}$

$\Rightarrow$ not a π-pulse

$$\begin{pmatrix} 1.6 & 2.0 & 3.6 & 93.2 \\ 5.9 & 95.1 & 23.8 & 1.6 \\ 1.8 & 0.6 & 37.2 & 3.7 \\ 91.7 & 3.9 & 35.4 & 2.7 \end{pmatrix}$$

$\uparrow$

$|1\rangle|1\rangle_{\text{ph}} \to \alpha\,|1\rangle|1\rangle_{\text{ph}} + \beta\,|0\rangle|2\rangle_{\text{ph}}$ not properly measured with the method.

with trapped, $^{88}Sr^+$, from J. Łabaziewicz PhD thesis (MIT, 2008)

Coupling ions via phonons

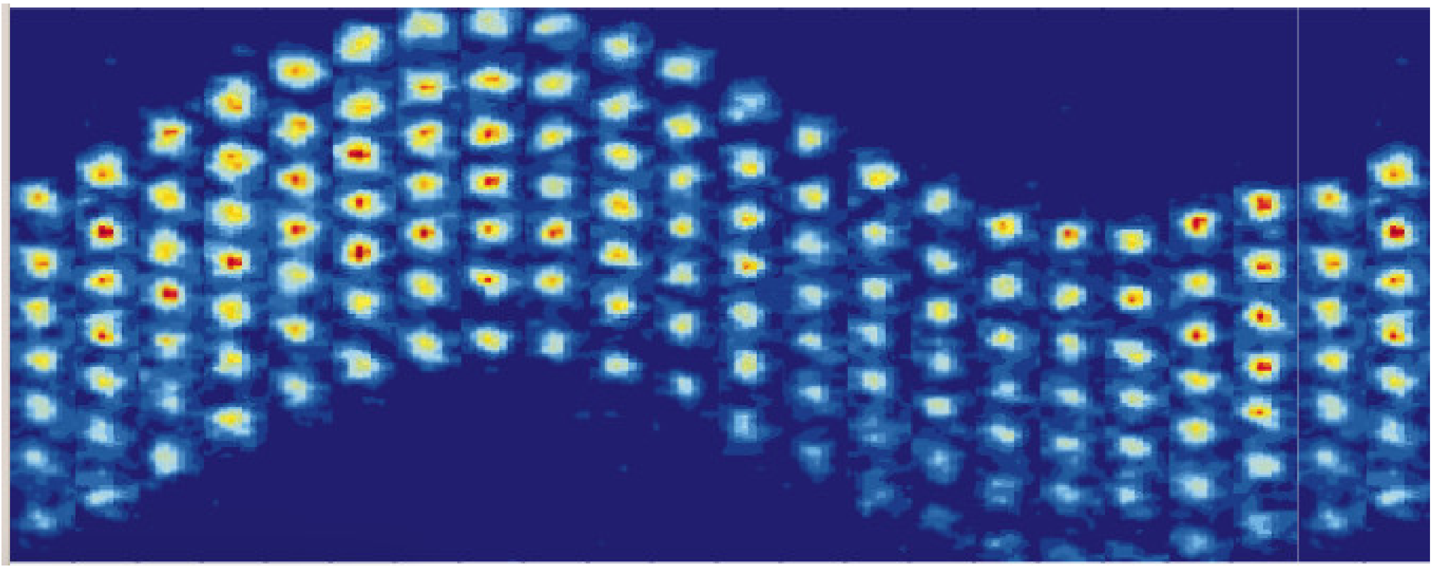

Using phonons as control qubit in a two-qubit gate

- Some transitions (BSB, RSB) are not allowed depending on the phonon excitation $\Rightarrow$ use this for 2-qubit gates with a control qubit.
- Possible with 1 ion (control = phonon, target = internal state) using an auxiliary internal state $|g'\rangle$ (or a subtle pulse sequence):

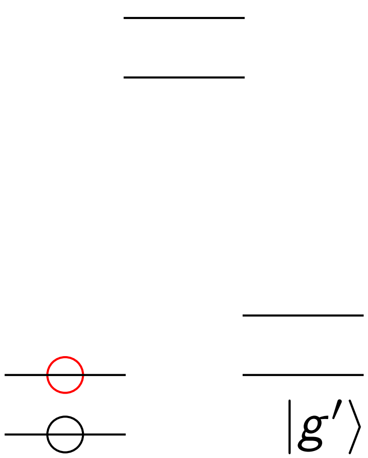

initial state

Using phonons as control qubit in a two-qubit gate

- Some transitions (BSB, RSB) are not allowed depending on the phonon excitation $\Rightarrow$ use this for 2-qubit gates with a control qubit.
- Possible with 1 ion (control = phonon, target = internal state) using an auxiliary internal state $|g'\rangle$ (or a subtle pulse sequence):

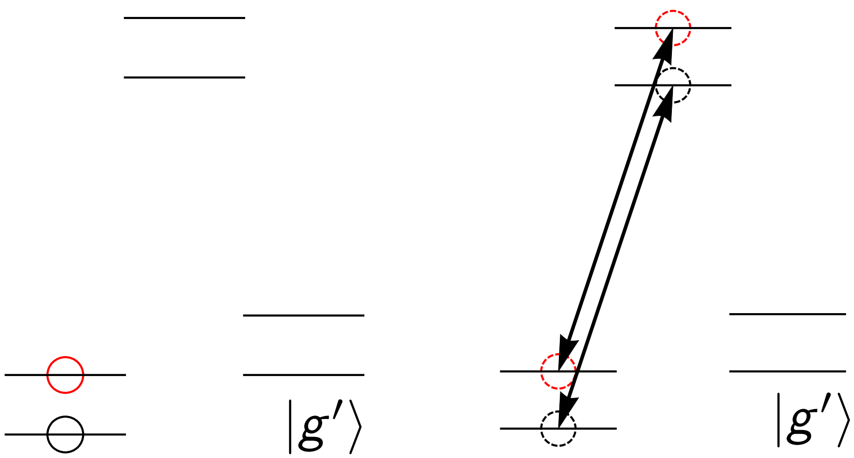

initial state

$+\pi/2$-carrier

Using phonons as control qubit in a two-qubit gate

- Some transitions (BSB, RSB) are not allowed depending on the phonon excitation $\Rightarrow$ use this for 2-qubit gates with a control qubit.
- Possible with 1 ion (control = phonon, target = internal state) using an auxiliary internal state $|g'\rangle$ (or a subtle pulse sequence):

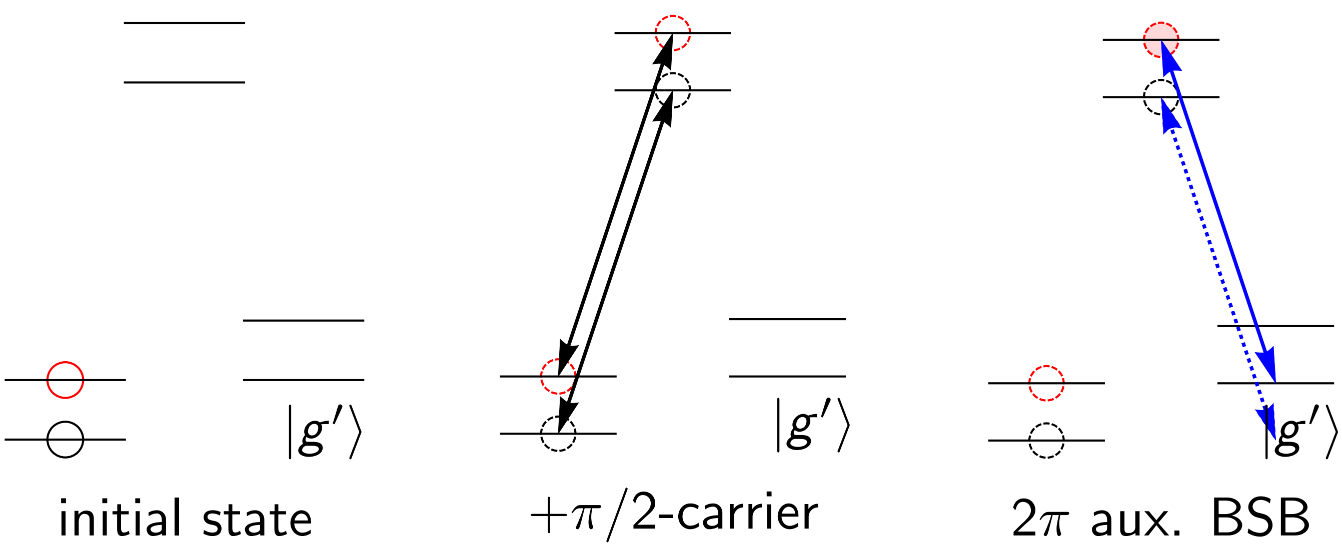

Using phonons as control qubit in a two-qubit gate

- Some transitions (BSB, RSB) are not allowed depending on the phonon excitation $\Rightarrow$ use this for 2-qubit gates with a control qubit.
- Possible with 1 ion (control = phonon, target = internal state) using an auxiliary internal state $|g'\rangle$ (or a subtle pulse sequence):

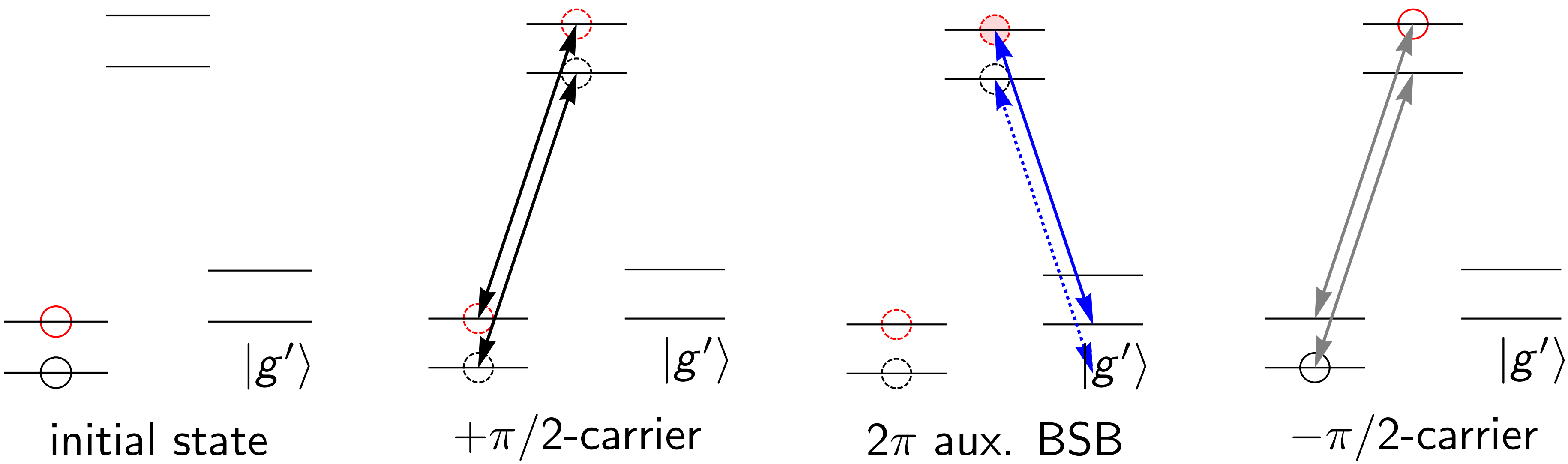

CNOT gate: second $-\pi/2$-pulse on carrier erases the effect of the first, unless a phase change has occurred with the BSB pulse to $|g'\rangle$.

$|x\rangle\,|0\rangle_{\rm ph} \to |x\rangle\,|0\rangle_{\rm ph}$ $\qquad |x\rangle\,|1\rangle_{\rm ph} \to |\mathrm{NOT}(x)\rangle\,|1\rangle_{\rm ph}$

Coupling ions via phonons

- Some transitions (BSB, RSB) are not allowed depending on the phonon excitation $\Rightarrow$ use this for 2-qubit gates with a control qubit.
- Possible with 1 ion (control = phonon, target = internal state)
- Even better with several ions, to implement algorithms with many qubits
- Ion chain in a linear Paul trap: collective motional modes
- The phonon excitation is **shared by all ions**

Ex with two ions in harmonic trap + Coulomb repulsion:

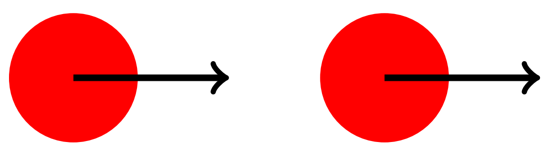

center of mass mode at ω_0

breathing mode at $\sqrt{3}\omega_0$

Normal modes of an ion chain

N ions, x_i: $x_1 < x_2 < \cdots < x_N$

Two forces: $-m\omega_0^2 x_i$ Coulomb force: $+\dfrac{q^2}{4\pi\varepsilon_0 (x_i - x_j)^2}\,\mathrm{sgn}(x_i - x_j)$

Coupled equations:

$$m\ddot{x}_i = -m\omega_0^2 x_i + \sum_{j<i} \frac{q^2}{4\pi\varepsilon_0 (x_i - x_j)^2} - \sum_{j>i} \frac{q^2}{4\pi\varepsilon_0 (x_i - x_j)^2}$$

→ collective modes.

center of mass mode: $X = \dfrac{1}{N}\displaystyle\sum_{i=1}^{N} x_i$

$$mN\ddot{X} = -mN\omega_0^2 X + \cancel{\frac{q^2}{4\pi\varepsilon_0}\sum_{i=2}^{N}\sum_{j=1}^{i-1}\frac{1}{(x_i - x_j)^2}} - \cancel{\frac{q^2}{4\pi\varepsilon_0}\sum_{i=1}^{N-1}\sum_{j>i}\frac{1}{(x_i - x_j)^2}}$$

$$\boxed{\ddot{X} = -\omega_0^2 X}$$

Expand coupled eq° close to equilibrium,

→ normal modes. Ex: $x_i = \lambda x_{i,eq}$ $\omega_B^2 = 3\omega_0^2$

Normal modes of an ion chain

Ex with 7 ions (H-C Nägerl thesis 1998):

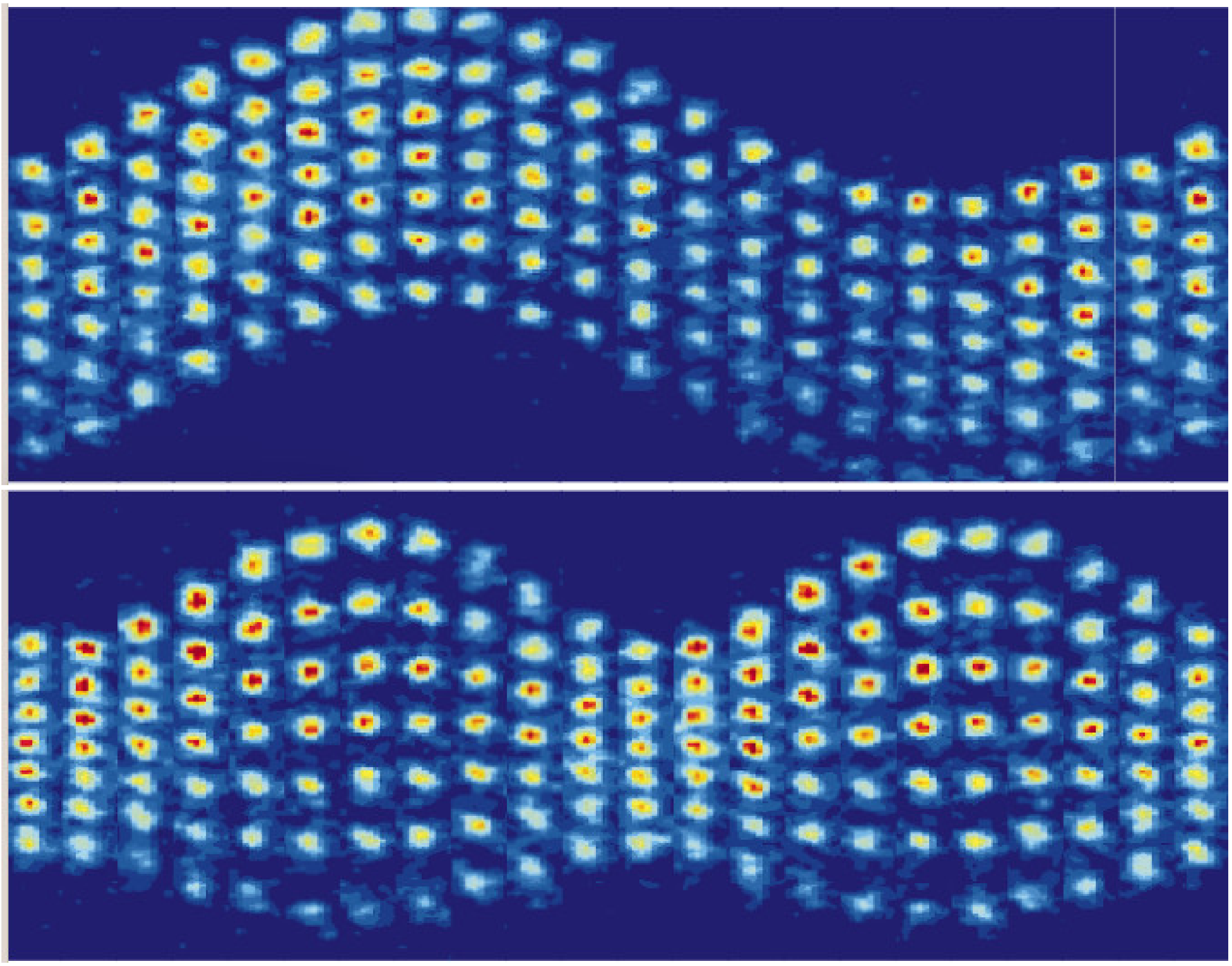

center of mass mode
at ω_0

breathing mode
at $\sqrt{3}\omega_0$

etc.

CNOT gate with two ions coupled by phonons

With laser-addressable ions

- The two ions share the same c.o.m. mode.
- Initialization in the common ground state of motion $|0\rangle_{\text{ph}}$.

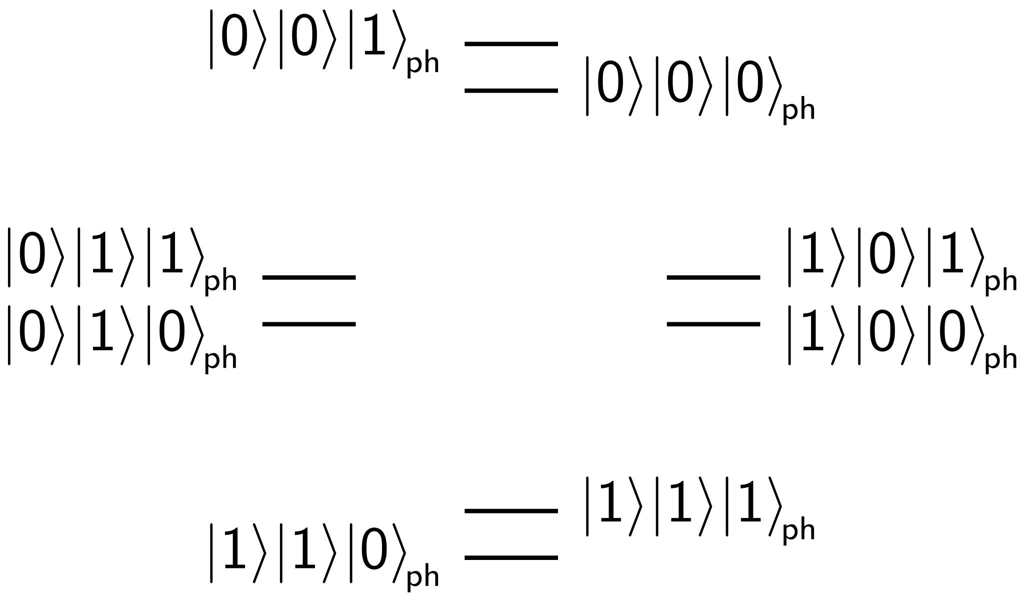

CNOT gate with two ions coupled by phonons

With laser-addressable ions

- The two ions share the same c.o.m. mode.
- Initialization in the common ground state of motion $|0\rangle_{\mathrm{ph}}$.
- π-BSB on ion 1 (control), only if in $|1\rangle$: $|1\rangle\,|x\rangle\,|0\rangle_{\mathrm{ph}} \leftrightarrow |0\rangle\,|x\rangle\,|1\rangle_{\mathrm{ph}}$

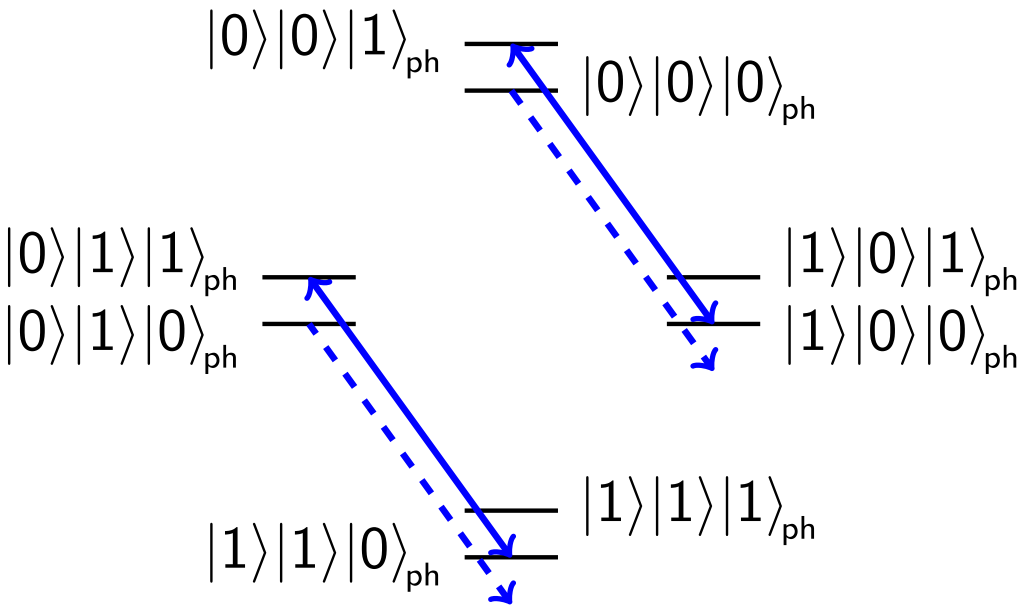

CNOT gate with two ions coupled by phonons

With laser-addressable ions

- The two ions share the same c.o.m. mode.
- Initialization in the common ground state of motion $|0\rangle_{\mathrm{ph}}$.
- π-BSB on ion 1 (control), only if in $|1\rangle$: $|1\rangle\,|x\rangle\,|0\rangle_{\mathrm{ph}} \leftrightarrow |0\rangle\,|x\rangle\,|1\rangle_{\mathrm{ph}}$
- CNOT on ion 2 controlled by motion (see above).

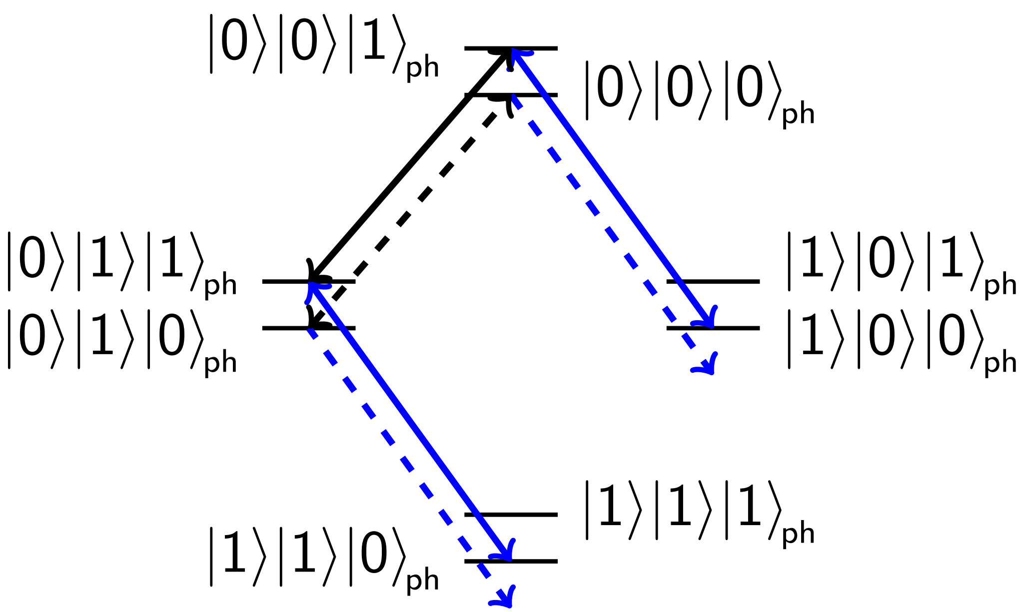

CNOT gate with two ions coupled by phonons

With laser-addressable ions

- The two ions share the same c.o.m. mode.
- Initialization in the common ground state of motion $|0\rangle_{\rm ph}$.
- π-BSB on ion 1 (control), only if in $|1\rangle$: $|1\rangle\,|x\rangle\,|0\rangle_{\rm ph} \leftrightarrow |0\rangle\,|x\rangle\,|1\rangle_{\rm ph}$
- CNOT on ion 2 controlled by motion (see above).
- π-BSB on ion 1: back to initial state for ion 1.

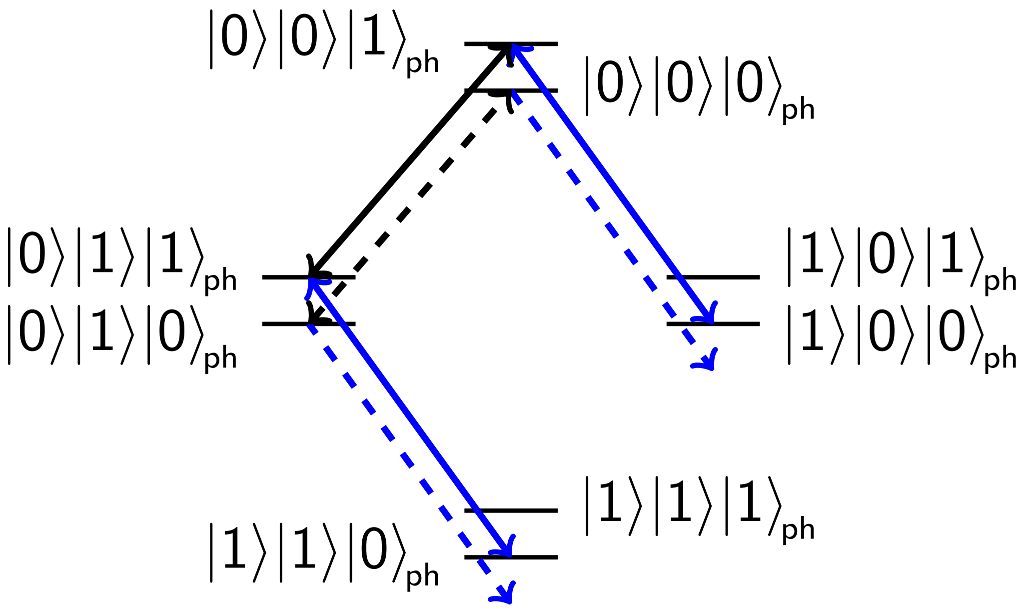

The scheme also works with $N > 2$ addressable ions.

Mølmer-Sørensen gate

Preparation of a Bell state

- Proposed by K. Mølmer and A. Sørensen, PRL **82**, 1971 (1999)
- Allows to prepare directly a Bell state $(|00\rangle - |11\rangle)/\sqrt{2}$
- Two-photon coupling from $|00\rangle$ to $|11\rangle$
- $\omega_r = \omega_{01} - \omega_0 - \Delta$, $\omega_b = \omega_{01} + \omega_0 + \Delta$
- Interference between paths $\Rightarrow$ coupling independent of n:

$$\Omega_{MS} = 2 \times \left[(n+1)\frac{\Omega_b\Omega_r}{2\Delta} + n\frac{\Omega_r\Omega_b}{-2\Delta}\right] = \frac{\Omega_r\Omega_b}{\Delta}$$

$$\frac{\Omega_1\Omega_2}{2\Delta}$$

Raman coupling for a 2-photon process

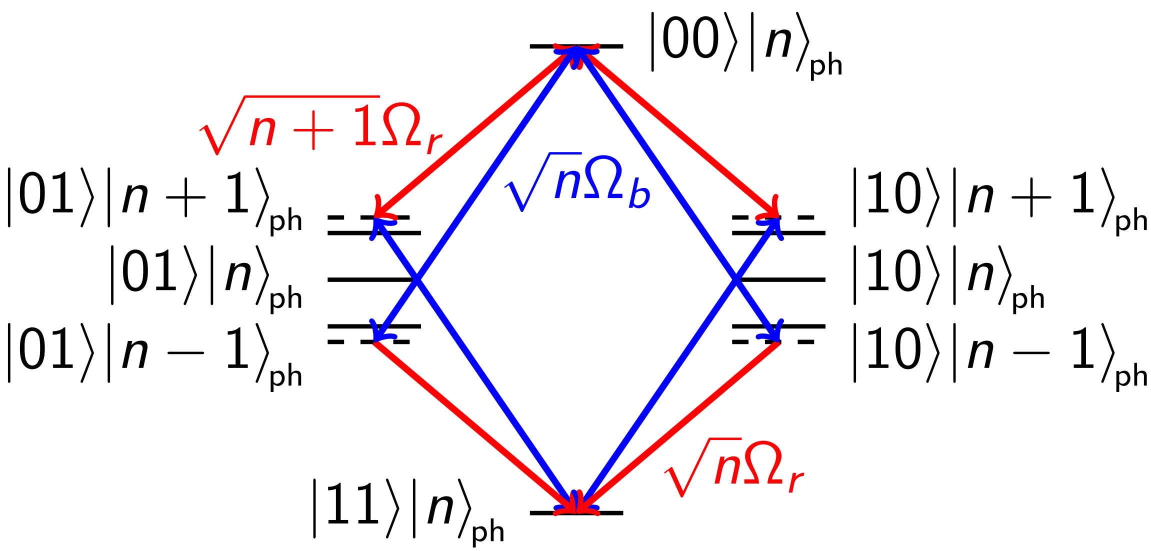

NB: $|01\rangle$ and $|10\rangle$ are coupled as well.

State-of-the-art single-qubit gate demonstrations

Type	Method	Fidelity	Time (μs)	Species	Ref.
1-qubit	Optical	0.99995	5	$^{40}\mathrm{Ca}^+$	Bermudez 2017
	Raman	0.99993	7.5	$^{43}\mathrm{Ca}^+$	Ballance 2016
	Raman	0.99996	2	$^{9}\mathrm{Be}^+$	NIST 2016
	Raman	0.99	0.00005	$^{171}\mathrm{Yb}^+$	Campbell 2010
	Raman	0.999	8	$^{88}\mathrm{Sr}^+$	Keselman 2011
	μwave	0.999999	12	$^{43}\mathrm{Ca}^+$	Harty 2014
	μwave		0.0186	$^{25}\mathrm{Mg}^+$	Ospelkaus 2011

Adapted from Bruzewicz et al.

State-of-the-art two-qubit gate demonstrations

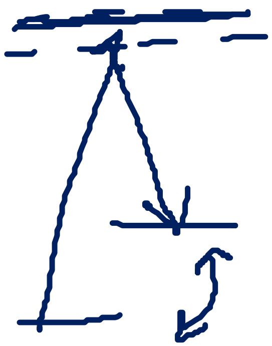

Type	Method	Fidelity	Time (μs)	Species	Ref.
2-qubit	Optical	0.996	–	$^{40}\mathrm{Ca}^+$	Erhard 2019
(1 sp.)	Optical	0.993	50	$^{40}\mathrm{Ca}^+$	Benhelm 2008
	Raman	0.9991(6)	30	$^{9}\mathrm{Be}^+$	NIST 2016
	Raman	0.999	100	$^{43}\mathrm{Ca}^+$	Ballance 2016
	Raman	0.998	1.6	$^{43}\mathrm{Ca}^+$	Schafer 2018
	Raman	0.60	0.5	$^{43}\mathrm{Ca}^+$	Schafer 2018
	μwave	0.997	3250	$^{43}\mathrm{Ca}^+$	Harty 2016
	μwave	0.985	2700	$^{171}\mathrm{Yb}^+$	Weidt 2017
2-qubit	Ram./Ram.	0.998(6)	27.4	$^{40}\mathrm{Ca}^+/^{43}\mathrm{Ca}^+$	Ballance 2015
(2 sp.)	Ram./Ram.	0.979(1)	35	$^{9}\mathrm{Be}^+/^{25}\mathrm{Mg}^+$	Tan 2015

Adapted from Bruzewicz et al.

Algorithms performed with trapped ions

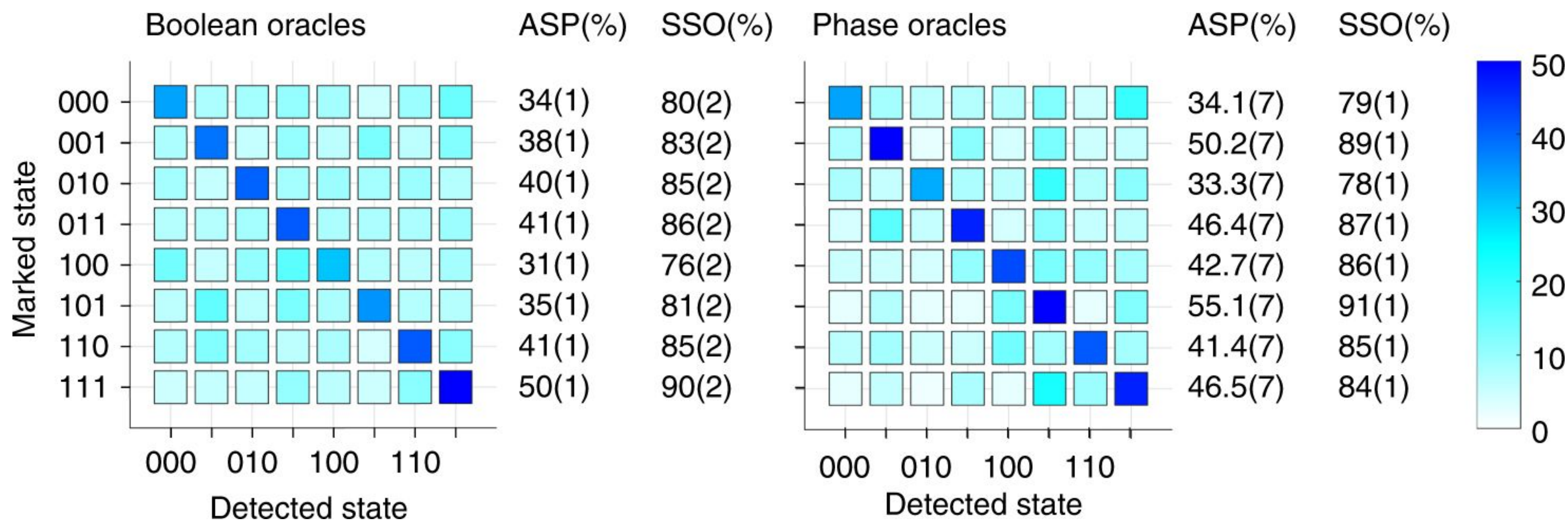

Results of Grover algorithm, Figatt et al., Nature Comm. **8**, 1918 (2017)

Algorithms implemented with trapped ions

The recent implementations were done by Monroe's group (Maryland) or Blatt's group (Innsbruck).

- Spin and phase flip error detection up to 7 ions [Nigg et al. Science **345**, 302 (2014)]
- Deutsch-Jozsa / Bernstein-Vazirani algorithm: determines if a $N \to 1$ operation is either constant or balanced ($3 + 1$ ions $+$ ancilla) [Debnath et al. Nature **536**, 63 (2016)]
- Quantum Fourier transform (QFT) (with 5 ions) [Debnath et al. ibid.]
- Grover's search algorithm (with 2 and 3 ions) [C. Figgatt et al., Nature Comm. **8**, 1918 (2017)]
- Shor algorithm (with 5 ions): $15 = 3 \times 5$ [Monz et al. Science **351**, 1068 (2016)]
- Variational quantum energy solver (VQE) applied to the ground state of H_2, LiH and H_2O (up to 11 ions) [C. Hempel et al., Phys. Rev. X **8**, 031022 (2018); Y. Nam et al., arXiv:1902.10171 (2019)]

Example: Deutsch-Jozsa algorithm

Implementation with 95% success rate on a 5-qubit computer

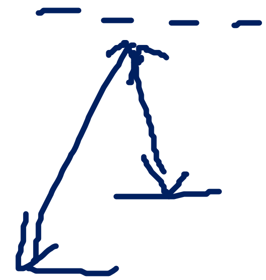

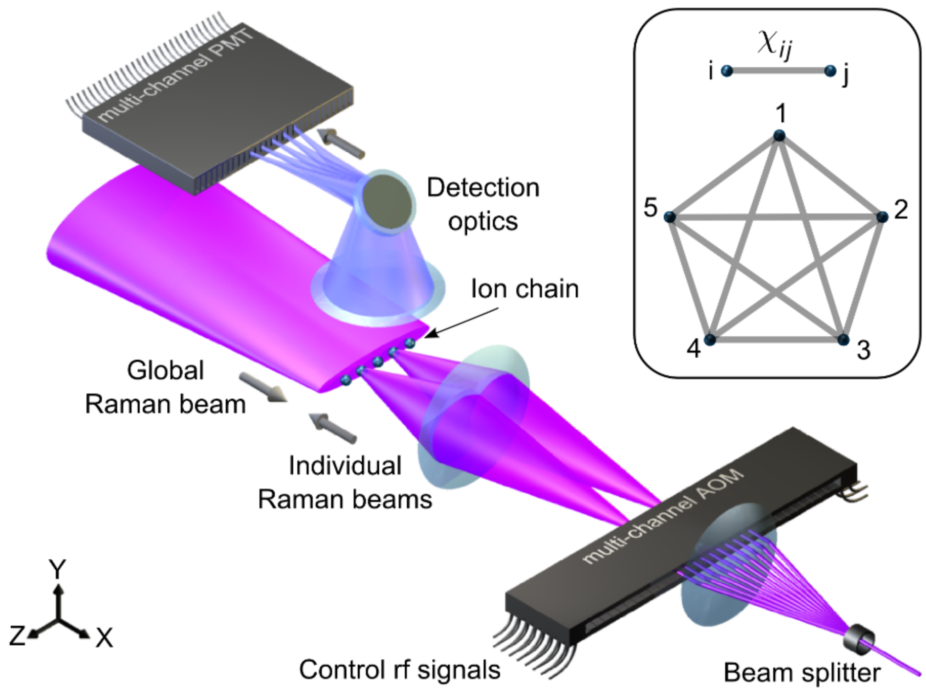

Experimental setup [Debnath et al. Nature **536**, 63 (2016)].

- 5 $^{171}\mathrm{Yb}^+$ ions
- Paul trap 3×0.27 MHz
- spacing 5 μm
- HF states $|F=0, m_F=0\rangle$ and $|F=1, m_F=0\rangle$, 12.6 GHz
- gates: Raman transitions
- $\tau_{\mathrm{coh}} > 0.5$ s
- single qubit detection $> 99\%$
- 5 qubits: 95.3% on average
- Deutsch-Jozsa: $|x\rangle$ with 3 qubits, 1 qbit for register, 1 ancilla

Example: Deutsch-Jozsa algorithm

Implementation with 95% success rate on a 5-qubit computer

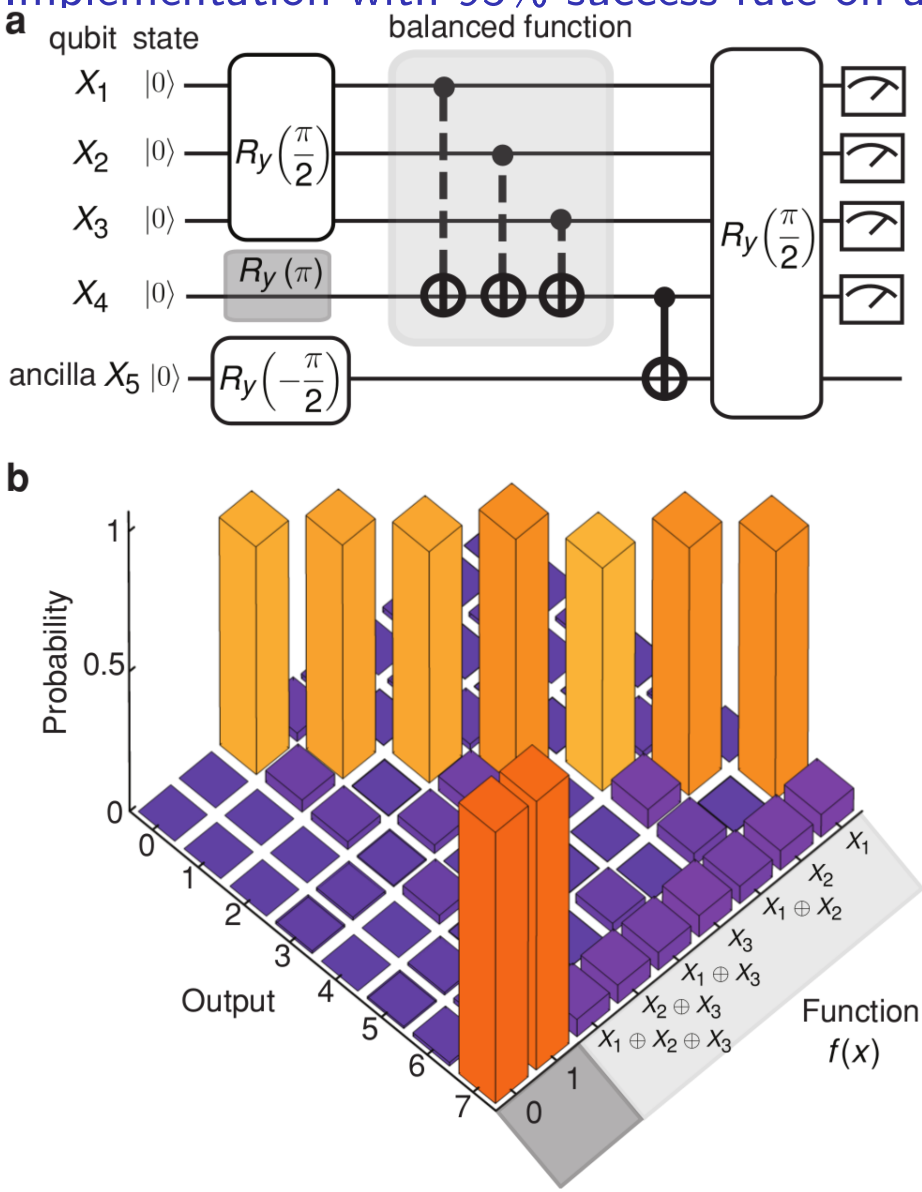

Algorithm:

1. Prepare equal superposition of all $|x\rangle$ and ancilla in $|a\rangle = (|0\rangle - |1\rangle)/\sqrt{2}$
2. Use C$_i$NOT(4) to apply $f(x)$:
$$\sum_x |x\rangle\, |f(x)\rangle\, |a\rangle$$
3. C$_4$NOT(5)
$$\sum_x (-1)^{f(x)}\, |x\rangle\, |f(x)\rangle\, |a\rangle$$
4. Last R_y brings the state in $(|y\rangle\,|0\rangle\,|0\rangle + |y'\rangle\,|1\rangle\,|0\rangle)/\sqrt{2}$ such that $f(x) = x \cdot \bar{y}$
5. Conditional meas. $X_4 = 0$: get $|y\rangle$ or $|111\rangle$

DiVincenzo criteria with a trapped-ion quantum computer

- A scalable physical system with well characterised qubits. **Scalability?**
- The ability to initialize the state of the qubits to a simple fiducial state. **OK with laser cooling and optical pumping, < 1 ms**
- Long relevant decoherence times. **OK with microwave transitions or narrow-line optical transitions, $>$ 100 ms**
- A universal set of quantum gates. **OK: single-qubit rotations with fidelity up to 99.9999% (microwave), CNOT up to 99.9%**
- A qubit-specific measurement capability. **OK with the shelving method, < 200 μs with fidelity 99.99%**

N.B. State preparation + readout with a fidelity 99.93% demonstrated, i.e. state preparation error $\sim 2 \times 10^{-4}$.

Source: Bruzewicz et al.

Efforts towards scalability

- Development of surface ion traps
- Having hundreds of addressable ions in a trap is 'easy'
- Difficult point: controlling their interation (with phonons)
- Possible solution: displace ions in a specific interaction zone
- Explored by Dave Wineland (NIST Boulder), Chris Monroe (Univ. Maryland and IonQ company), ...

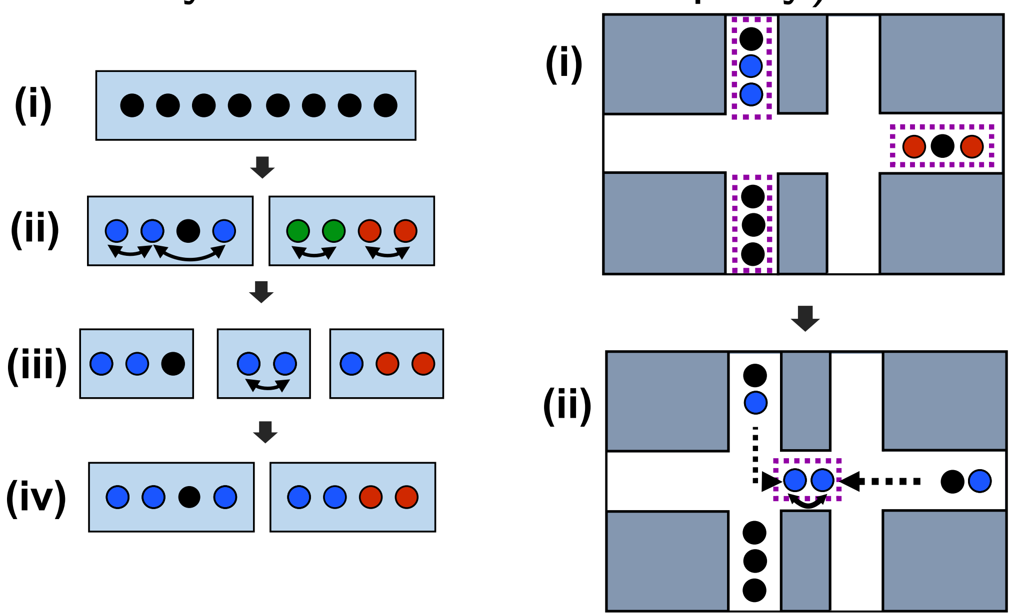

Fig. from Bruzewicz et al.

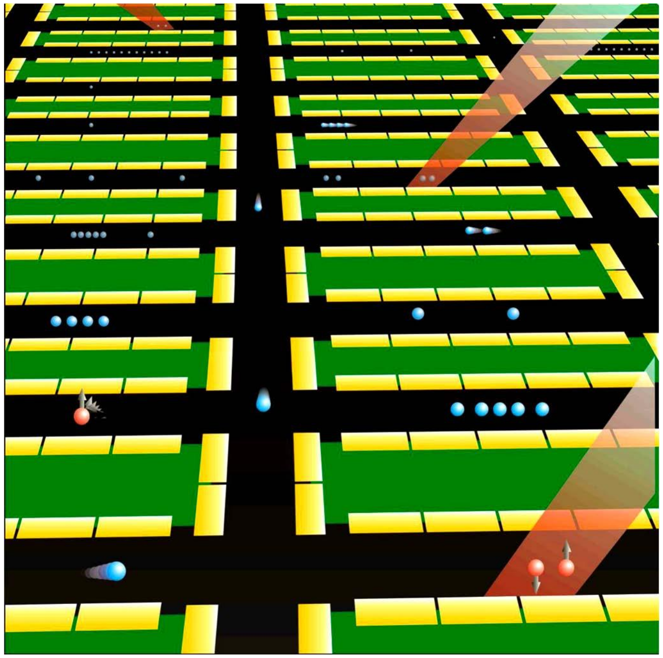

Fig. from NIST

Progress in optics integration

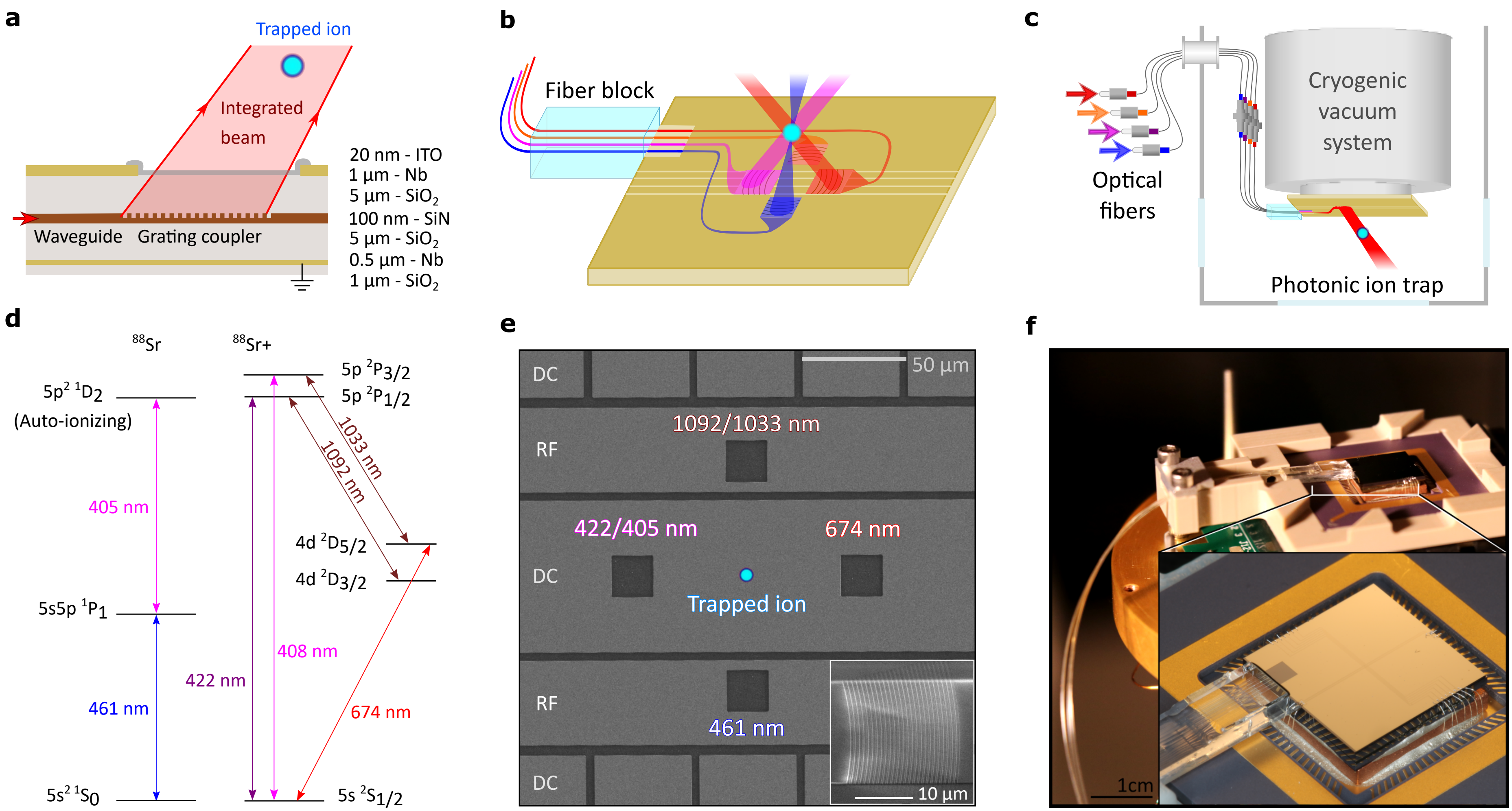

Fig. from Niffenegger et al., Nature **586**, 538 (2020) / arXiv:2001:05052

Bibliography for Lecture 1

- G. Benenti, G. Casati and G. Strini, *Principles of Quantum Computation and Information* vol. 2, World Scientific 2007
- C. Cohen-Tannoudji and D. Guéry-Odelin, *Advances in atomic physics: an overview*, World Scientific 2012 (or the French version, Hermann 2016)
- S. Haroche and J.-M. Raimond, *Exploring the quantum*, OUP 2006
- C. Champenois, *Trapping and cooling of ions*, Les Houches lecture notes `https://cel.archives-ouvertes.fr/cel-00334152`
- D. Leibfried, R. Blatt, C. Monroe, and D. Wineland, *Quantum dynamics of single trapped ions*, Reviews of Modern Physics **75**, 281 (2003)
- C. Bruzewicz et al., *Trapped-Ion Quantum Computing: Progress and Challenges*, Appl. Phys. Rev. **6**, 021314 (2019) `https://arxiv.org/abs/1904.04178`
- P. Schindler et al., *A quantum information processor with trapped ions*, New Journal of Physics **15**, 123012 (2013)
- S. Debnath et al., *Demonstration of a small programmable quantum computer with atomic qubits*, Nature **536**, 63 (2016)